UNIVERSITY OF GOTHENBURG

DEPARTMENT OF BIOLOGICAL AND ENVIRONMENTAL SCIENCES

Investigation of Ice Nucleating Particles (INPs) in southern Sweden

With a special focus on their origin, possible connection to meteorological parameters and aerosol properties

Malin Forsmalm

Degree project for Master of Science (120 hec) with major in Atmospheric sciences, climate and ecosystem
ES2521, Master Thesis in Atmospheric science with orientation towards Environmental Sciences, 60 hec
Second cycle
Semester/year: Autumn 2022, Spring 2023
Supervisor: Erik Thomson, Department of Chemistry and Molecular Biology
Co-Supervisor: Markus Hartmann, Department of Chemistry and Molecular Biology
Examiner: Xiangrui Kong, Department of Chemistry and Molecular Biology

Investigation of Ice Nucleating Particles (INPs) in southern Sweden

With a special focus on their origin, possible connection to meteorological parameters and aerosol properties

Malin Forsmalm

UNIVERSITY OF
GOTHENBURG

Gothenburg, Sweden 2023

Investigation of Ice Nucleating Particles (INPs) in southern Sweden
Malin Forsmalm

Supervisor: Erik Thomson, Department of Chemistry and Molecular Biology, University of Gothenburg
Co-supervisor: Markus Hartmann, Department of Chemistry and Molecular Biology, University of Gothenburg
Examiner: Xiangrui Kong, Department of Chemistry and Molecular Biology, University of Gothenburg

Department of Biological and Environmental Sciences
Gothenburg, Sweden 2023

Cover picture: Ice crystal (Aaron Burden, Unsplash, 2016).

Software system: LaTeX
Published by University of Gothenbrug
Gothenburg, Sweden 2023

Investigation of Ice Nucleating Particles (INPs) in southern Sweden

With a special focus on their origin, possible connection to meteorological parameters and aerosol properties

Malin Forsmalm
Department of Biological and Environmental Sciences

Abstract

This study investigates if there is a seasonal variability of ice nucleating particle (INP) concentrations. There is also a focus in seeing if there are correlations between meteorological parameters and aerosol properties and the measured INP concentrations.
The samples were collected from the research station Hyltemossa located in southern Sweden. Air was pumped through filters which trapped the particles. These filters were then transported to the University of Gothenburg where they went through an analysis to investigate the INP concentration. The method used for this investigation has been the Lund University Cold Stage (LUCS), which is a droplet freezing assay (DFA). With this method the sample solution droplets undergoes a controlled freezing process in an environmental chamber and the droplets freezing temperatures are registered. The information from this process is then utilized to retrieve the INP concentration for each sample.
The results from the study do not show any seasonal variations during the investigated time period. There are not any strong correlations between the INP concentrations and the meteorological parameters and aerosol properties that could be found either.

Keywords: INPs, DFA, LUCS

Sammanfattning

Det här arbetet presenterar en studie om det finns en säsongsvariation av iskristallbildande partiklars ("ice nucleating particles") (INP) koncentrationer. Det finns också ett fokus på om det finns några korrelationer mellan meteorologiska parametrar och aerosol egenskaper och de uppmätta INP koncentrationerna.
Proverna samlades in från forskningsstationen Hyltemossa som är belägen i södra Sverige. Luft pumpades igenom filter där partiklar fångades. Dessa filter transporterades sedan till Göteborgs Universitet där de genomgick an analys för att undersöka INP koncentrationen. Metoden som använts för den här studien har varit "Lund University Cold Stage" (LUCS) vilket är en droppfrysmetod. Med den här metoden så genomgår provlösningsdropparna en kontrollerad frysprocess i en klimatkammare och dropparnas temperatur vid frysningen registreras. Informationen från den här processen används sedan för att få fram INP koncentrationen för varje prov.
Resultaten från studien visar inte på några säsongsvariationer under den studerade tidsperioden. Det fanns inte heller några starka korrelationer mellan INP koncentrationer och meteorologiska parametrar och aerosol egenskaper som kunde konstateras.

Acknowledgement

First I want to thank everyone in the ice group for helping me when I had questions. A special thank you to my supervisor Erik Thomson and co-supervisor Markus Hartmann for guiding me through the process of my thesis work. I am also grateful for the opportunity to go to Andøya and experience some field work and other laboratory processes.

Malin

Contents

List of Figures

List of Tables

1

Introduction

The processes that occur in clouds around the Earth's atmosphere are important for weather and climate. Aerosols present in the atmosphere can have large effects when it comes to their interaction with the atmosphere. One of these interactions are reflection of the incoming solar radiation, which creates a cooling or warming effect on the atmosphere. Another is the aerosol cloud interaction which will have an effect on cloud properties like their lifetime and albedo. [1] The weather and climate will affect aspects like precipitation distribution and the energy balance of Earth [2] [3]. Even though clouds play an important role in regards to Earth their processes still holds large uncertainties when looking at climate models [3]. One type of clouds are so called mixed phase clouds (MPCs) where there is a co-existence of supercooled liquid and ice crystals. The formation of the ice crystals are triggered in the clouds by so called ice nucleating particles (INPs) which is the reason for the co-existing of the liquid droplets and ice crystals. [4] INPs are a subset of aerosol particles and have the ability to catalyze the ice formation process at a temperature range between 0 to -38 °C (Chapter 2.3). They can also effect the clouds microphysical and optical properties [3] [5]. Generally the concentration of INPs that can initiate freezing increases with decreasing temperature [3]. Since there is a large variation of atmospheric conditions, INPs effect on parameters such as cloud properties are hard to define but could be useful in predicting processes of ice formation and also with the development of climate models [6].

This study investigates seasonal variability of the INP concentration derived from collected filter samples. The samples were gathered from the Hyltemossa ACTRIS research station situated in the south of Sweden, see Chapter 3.1. The collected filter samples represent time periods between August to September (2021) and November (2022) to January (2023). Additionally, data from already collected and measured filter paper samples (March to July, 2021) will be investigated to build a longer time series. A Droplet Freezing Assay (DFA) was used to analyze the samples collected (Chapter 3.2). The DFA is able to give information to help calculate the concentration of INPs over a relevant temperature range. To be able to get further insight in how the concentration of INPs might be influenced, data from some meteorological parameters measured at Hyltemossa was used. Back trajectories, see Chapter 4.2, were also analyzed to see if there might be a connection between the air masses movement and INP concentration.

1.1 Aim

The aim of this thesis is to:

- Characterize aerosol filters for INP concentration.
- Investigate INP variability over time.
- Assess correlations between INP concentrations and other meteorological and aerosol properties.
- Relate INP measurements to air mass origin via back trajectory analysis.

2

Background

2.1 Aerosol particles

In Earth's atmosphere there are not only gases present but also small particles in the form of liquids and solids. The suspension of particles in a gas is called an aerosol and the particles are called aerosol particles. These small particles can have a large effect on processes that occur in the atmosphere. Which in turn has an effect on human health, the climate and weather of Earth. Because of these effects it is important to understand how the aerosol particles interact with its surrounding to be able to develop better climate models. [7]

The aerosol particles in the atmosphere interact with incoming solar radiation. [8] They will either scatter or absorb the radiation which in turn will give a cooling or warming effect of the atmosphere, this will be described more in Chapter 2.1.1. They will also play an important role when it comes to the formations of clouds, which will be described in Chapter 2.2. [9] Aerosol particles can originate from many different sources that both are natural and anthropogenic [10]. Some examples of the natural sources of aerosol particles can be dust storms, volcanic eruptions, wild fires and sea spray. Examples of anthropogenic sources are combustion, road transport and farming [1] [9] [11]. In Figure 2.1 there is an overview of some of the sources of the aerosol particles that end up in the atmosphere. It also shows what kind of effects they can have on the climate system and what changes that can result in [1].

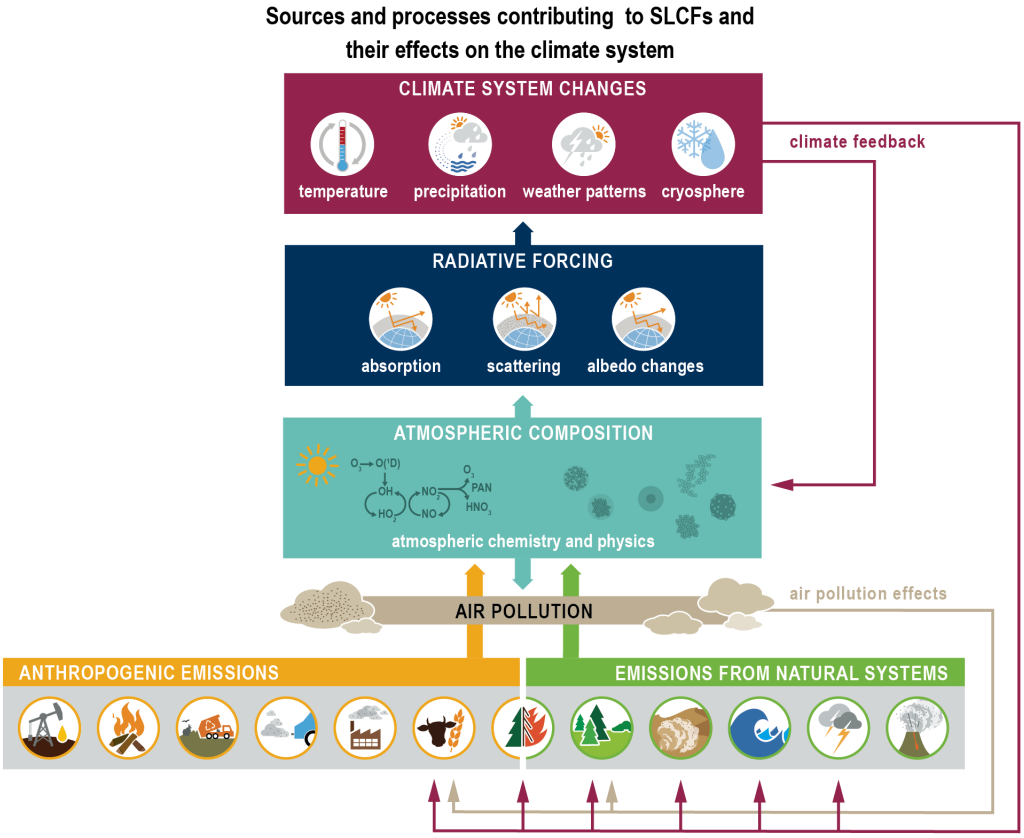

Figure 2.1: Overview of how different sources of aerosol particles end up in the atmosphere and how they will interact with their surrounding and have an effect on the climate. Where SLCFs stands for Short-Lived Climate Forcers. Figure reproduced from [1].

Since there are many different sources of aerosol particles their sizes can range from $0.001\mu m$ to $100\,\mu$m [10]. There will also be a variation in both shape and chemical composition which will have an effect on how they react with their surroundings. Some of the aerosol particles and their sizes can be found in Table 2.1.

Table 2.1: A selection of aerosols and their respective size ranges.

Aerosol particle	Size
Black carbon	$< 2.5\mu m$ [12]
Sea salt	$0.05\mu m$-$10\,\mu$m [13]
Dust	$1\,\mu$m-$100\,\mu$m [14]
Sulphate	<200 nm-$6\,\mu$m [15] [16]

Aerosol particles can also be divided into two types, primary and secondary aerosols. Primary aerosols are directly released in the atmosphere and are created through dispersion processes, such as volcanic ash and sea spray [17]. Secondary aerosols are instead formed in the atmosphere through atmospheric mechanisms, for example sulphates which are generated from burning of fossil fuels. [1] [9] The secondary particles are generated by nucleation in the atmosphere. Aerosol particles has a highly variable lifetime in the atmosphere. Their lifetime in the troposphere is up to about two weeks and in the stratosphere it has a lifetime of about a year. How long a specific type of aerosol will stay in the atmosphere depends mostly on the particles size. [18]

2.1.1 Aerosol particles and Climate

Aerosol particles in the atmosphere will either scatter or absorb incoming solar radiation. The aerosol particles that are in the troposphere will mainly scatter radiation, resulting in a cooling effect. The aerosol particles can also enhance cloud reflectance which has the indirect effect of cooling. [8] The aerosol particles can not only enhance the cloud reflectance but also the lifetime of the cloud. Both the direct and indirect aerosol effect will have an overall cooling effect on the climate [17]. This means that when more aerosol particles are released to the atmosphere a stronger overall cooling effect of the climate will occur, this can be seen in Figure 2.2 which is from the sixth IPCC report [19].

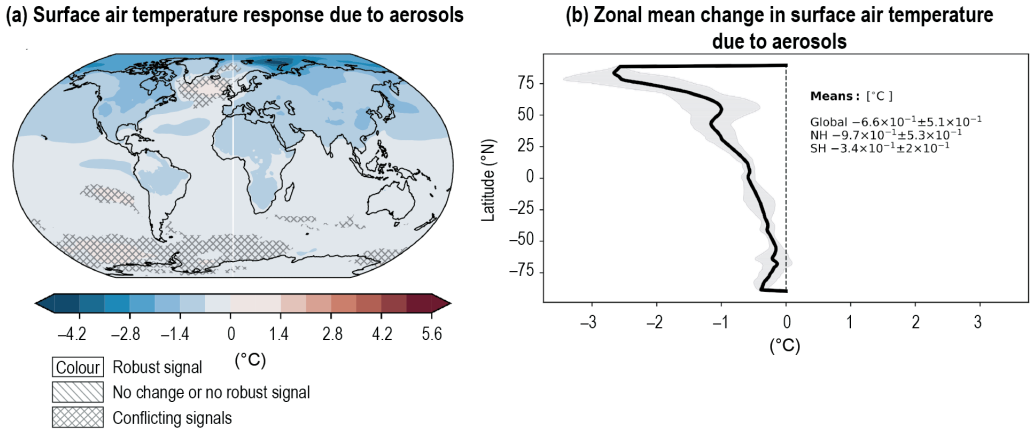

Figure 2.2: Overview of how the surface and zonal mean change air temperature are effected by aerosol particles in the atmosphere. Figure reproduced from [19].

2.2 Cloud formation

Aerosol particles are important for cloud formation, this is due to the fact that some of them have the properties of being a cloud condensation nuclei (CCN) or Ice Nucleating Particles (INPs). CCNs act as a nucleation site on which water vapour condenses and therefore can form liquid cloud droplets. [20] Some aerosol particles will have the properties of being ice nucleating particles (INPs) which will act as a nucleating site for the forming of ice crystals, which will be described in Chapter 2.3.

With a large concentration of CCN in the atmosphere it is more likely that smaller droplets will be formed. Clouds with smaller droplets in them tend to look more white and have a longer lifetime. In addition to them being whiter they will also have an enhanced reflectance. If you instead look at the opposite, with a smaller concentration of CCN, cloud droplets tend to be bigger and therefore the clouds will appear more grey and have a shorter lifetime and not the same enhanced reflectance.

There are two types of clouds formed in the troposphere where ice is present, these two are cirrus clouds and mixed phase clouds (MPCs). Clouds situated in the middle and the low troposphere are the ones that have an important impact on Earth's climate. At these altitudes and with a temperature range of 0 to -37 °C you can find MPCs. [21] [20] In MPCs there is a co-existence of the waters three stages of matter, water vapour, water droplets that are supercooled and ice crystals. This type of cloud can be found at all latitudes and therefore their processes are important for predictions of Earth's weather and climate. Despite holding an important role in Earth's weather and climate there is still a gap in the understanding how MPCs behave. [22] With this gap of knowledge MPCs influences on the climate gives an uncertainty in today's climate models [23] [22]. Especially when it comes to the interaction of the clouds and the aerosol particles present in the atmosphere. The CCN and INPs present in clouds have, as stated, an effect on the clouds that is important to understand when it comes to the development of climate models. As seen in Figure 2.3 there is still a large uncertainty when it comes to aerosol interaction with clouds and radiation [24].

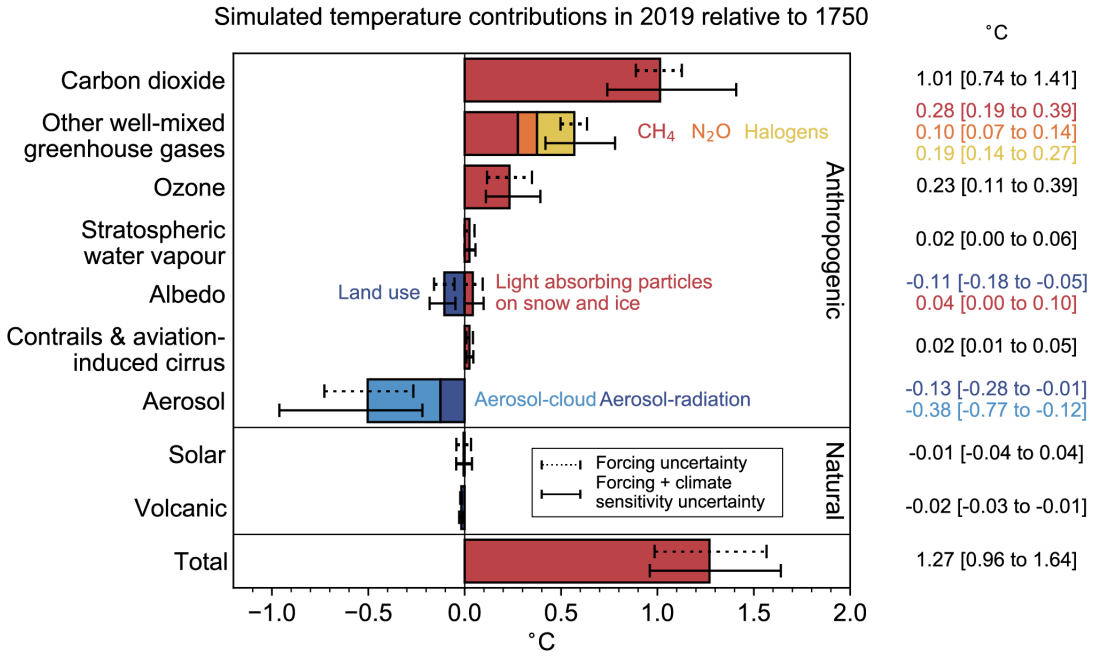

Figure 2.3: Simulated temperature contributions between the year 2019 in comparison to 1750 for different forcing agents. Figure reproduced from [24].

When the amount of aerosol particles change so will the properties of clouds as well as stated earlier. Understanding how aerosol particles interact with both clouds and radiation is an important part of being able to develop accurate climate models in the future.

2.3 Ice nucleation

Ice is formed in clouds with the help of ice nucleating particles (INPs) as the catalyst. There are two types of ice formation processes, homogeneous ice nucleation and heterogeneous ice nucleation. Homogeneous ice nucleation will form ice crystals with liquid droplets without any other particles present. The ice formation due to homogeneous ice nucleation usually occur in temperatures at or below -38°C. [25] In this thesis homogeneous ice nucleation is not an investigated mechanism unlike the heterogeneous ice nucleation, therefore there will not be a more thorough description of this process. Heterogeneous ice nucleation on the other hand occur with the help of ice nucleating particles. The heterogeneous ice nucleation can be described by different modes to go from a liquid droplet to an ice crystal which is described in Chapter 2.3.1. The temperature range for ice formation through heterogeneous ice nucleation in clouds is usually between 0 and -38°C [5].

2.3.1 Heterogeneous ice nucleation

Heterogeneous ice nucleation occurs when ice crystals form with the help of INPs. The different modes in mixed phase clouds of heterogeneous ice nucleation are [21]:

- Deposition nucleation
- Immersion freezing
- Condensation freezing
- Contact freezing

These four different modes of how ice is formed through heterogeneous ice nucleation are illustrated in Figure 2.4.

Deposition nucleation is the process where ice is formed in an environment where supersaturated vapour is present. The supersaturated vapour will settle as ice onto a solid particle surface, which will be the ice nucleating particle. This will then form ice crystals.

For immersion freezing the INP will be suspended in a supercooled liquid droplet. The liquid droplet will go through some cooling and ice will then nucleate on the INP that is encased by the liquid droplet.

For the case of condensation freezing the solid particle will have water vapour that condenses on it. The condense will then freeze on the INP. This mode is sometimes also classed together with the two previous mentioned modes.

The last mode to mention is contact freezing this is when there is a supercooled liquid droplet that collides with a supercooled solid particle, and after the collision initiates ice formation [26] [21].

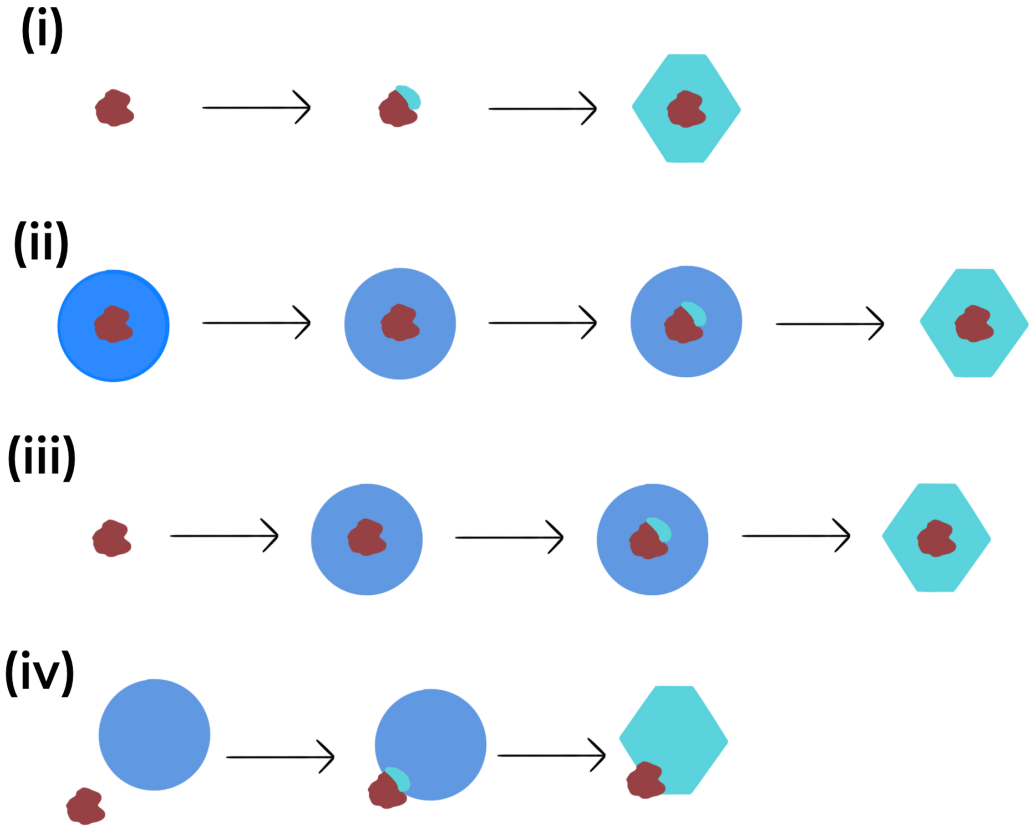

Figure 2.4: Here is the four different heterogeneous ice nucleation modes shown. It shows how a water droplet and a ice nucleating particle interact to form an ice crystal. (i) Deposition nucleation - supersaturated vapour settle on a solid particle in the form of ice. (ii) Immersion freezing - A solid particle is suspended in a liquid droplet that goes through cooling before ice starts forming on the particle. (iii) Condensation freezing - Water vapour condenses on the solid particle and it will then form ice on the particle. (iv) Contact freezing - A supercooled liquid droplet and a supercooled solid particle will come in contact and will then start forming ice. [27] [26]

Ice nucleating particles catalyze the heterogeneous ice formation process as mentioned previously. The aerosol particles that can act as INPs come from several different sources that both are natural and anthropogenic, which is described in Chapter 2.1 and some of these are listed in Table 2.1. From the freezing temperature you can get an indication of which type of INPs are present. This can be seen in Figure 2.5 where the ice active site density (taken from data from literature), which here is denoted as n_s, is plotted against the temperature to see the different INPs ice nucleating efficiency [21].

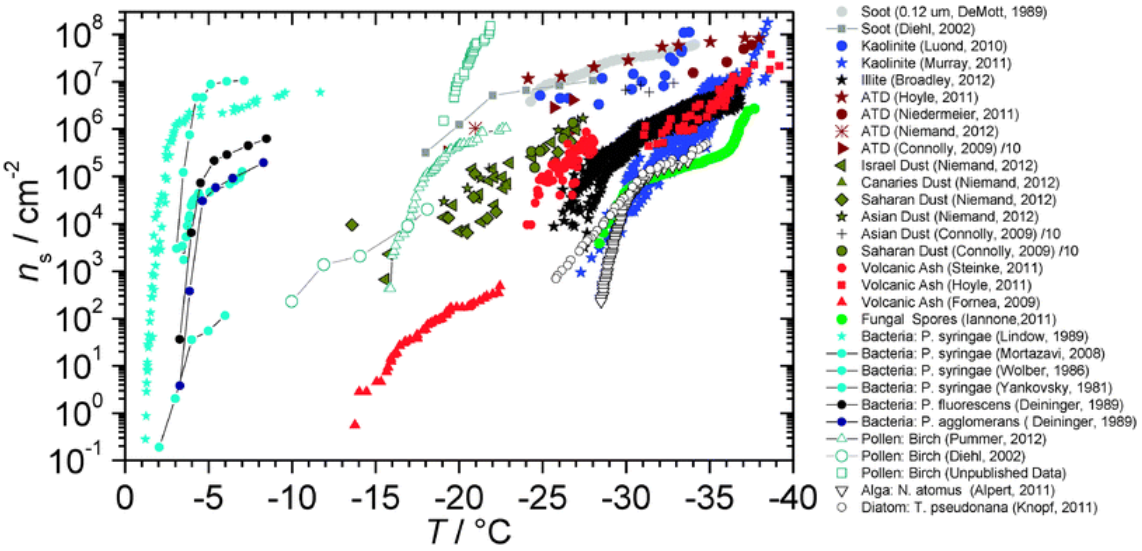

Figure 2.5: The ice nucleating efficiency of different types of INPs. Figure reproduced from [21].

Figure 2.5 shows that aerosol particles from biological materials, bacteria and pollen, act as INPs mostly at temperatures from -20°C and above. At temperatures of -15°C and below the materials that dominate are instead mineral dust and soot.

3

Methods

3.1 Hyltemossa Research Station

Hyltemossa research station is, as can be seen in Figure 3.1, located in the south of Sweden (about 56 km north of Lund). The research station is located in managed forest with Norwegian spruce as main tree species [28]. The level of pollution here is typically low but depending on outside factors like meteorological phenomenons and where air masses comes from the level of pollution can vary [29]. Hyltemossa is a co-location for both atmosphere and ecosystem research where ACTRIS (The Aerosol, Clouds and Trace Gases Research Infrastructure) and ICOS (Integrated Carbon Observation System) have funded the infrastructure that exists at the location. [28] [29]

It is from this location the samples used in this study is collected from. The sampling equipment used is a Leckel sampler that is mounted on a tower where continues sampling takes place. It is set up with a PM_{10} inlet and an air flow rate of $1\,\mathrm{m^3h^{-1}}$. [30] The filter samples are then transferred frozen to the University of Gothenburg for analysis. To analyze the filters a Droplet Freezing Assay (DFA) is used which is described in Chapter 3.2.1.

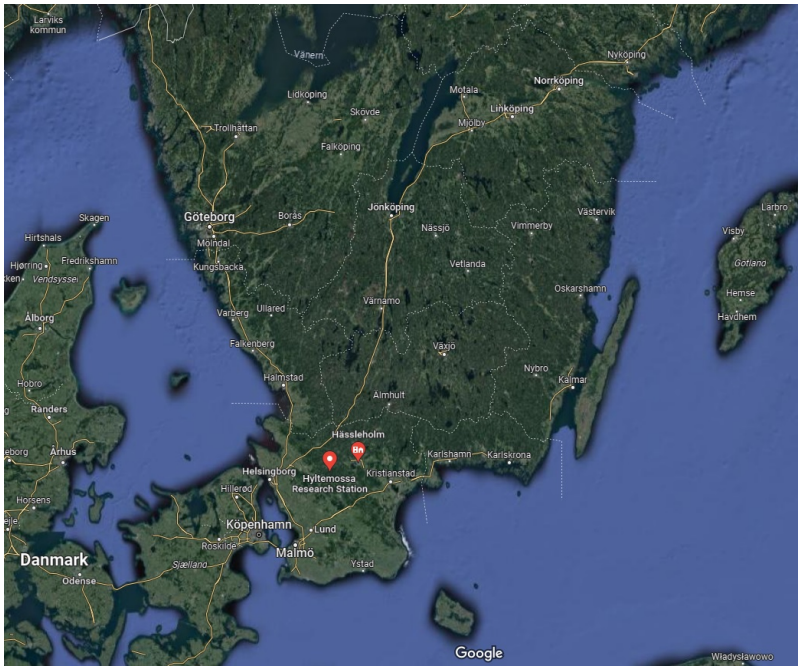

Figure 3.1: Map of the location of Hyltemossa Research Station in the southern part of Sweden. It also shows the location of Hässleholm where pollen data is recorded. The distance between Hyltemossa research station and Hässleholm is $\approx 23\,\text{km}$ [31].

3.2 Experiment

3.2.1 Experimental setup

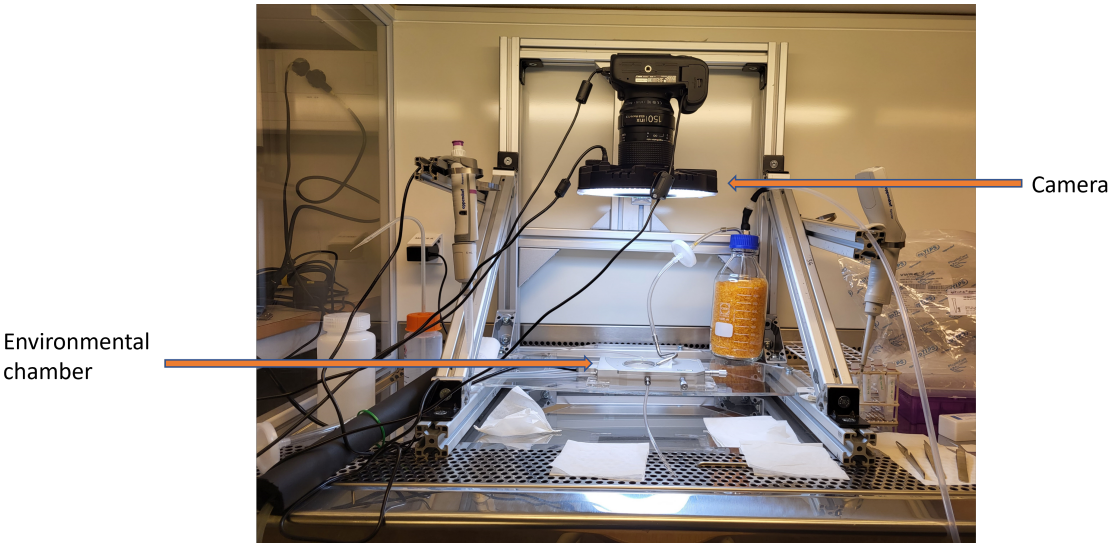

Figure 3.2: An overview of the experimental setup used during the experiments done for this thesis. Which shows the placement of the camera and the environmental chamber.

Figure 3.2 shows an overview of the experimental setup that was used to observe the freezing of the water droplets. This method is called Droplet Freezing Assay (DFA) and is a technique that has been used for some time. [32] The basic of this technique is that droplets are placed on a surface with a spacer that will keep the droplets separated. The droplets will then undergo a decrease of temperature until freezing occurs. From the information gained from the freezing process with already known information about the sampled air volume, volume of wash water and droplet volume the concentration of INP can be retrieved. [2] [6] In this experiment the DFA that is used is a cold stage setup called LUCS (Lund University Cold Stage) which is a setup that has taken inspiration from several other cold stage setups [33]. The schematic of this cold stage setup can be seen in Figure 3.3.

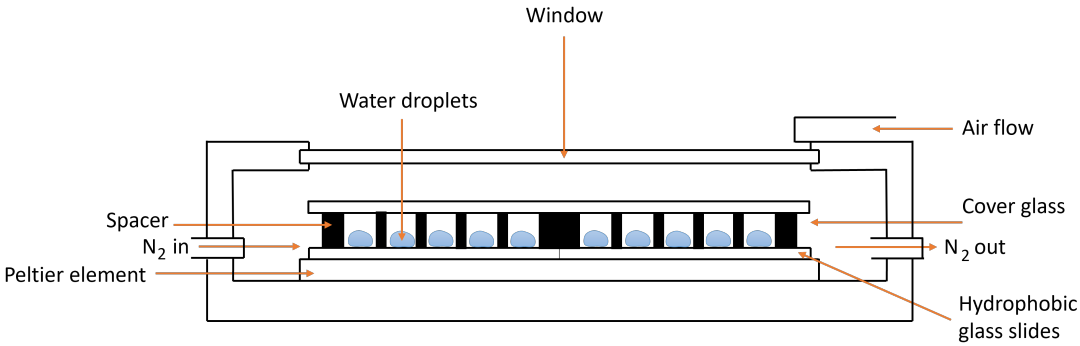

Figure 3.3: A schematic figure of the environmental chamber with the cold stage that is seen in the setup in Figure 3.2

3.2.2 Sample preparation and experimental procedure

The filter samples goes through a sample preparation procedure before the droplets get placed on the cold stage in the environmental chamber. To avoid contamination all equipment is sterilised before use and gloves are changed during the experiments. The first step is to cut the filter sample in half. Half of the filter is transferred to a sample vial to which 2 ml of purified water is added. The vial is then placed on a vortex mixer where it is shaken for ≈ 5 minutes.

Four hydrophobic glass slides are placed on the peltier element and on top of that the spacer will be placed. This can be seen in Figure 3.4. The spacer that lies between the hydrophobic glass slides and the cover glass (which can be seen in Figure 3.3) allows each droplet of water to be separated while on the cold stage. The pattern of this mesh can be seen in Figure 3.4a. Each droplet of 1 μl sample will be placed in each of these hexagonal shapes. In total there will be 100 drops each time. A cover glass will then be placed on top of the spacer before the environmental chamber is closed. On top of the environmental chamber there will be an air flow and nitrogen will go through it to help to avoid that the window of the chamber will develop condensation and fog up. Above the chamber a camera is placed (as seen in Figure 3.2) that records images as the stage is cooled.

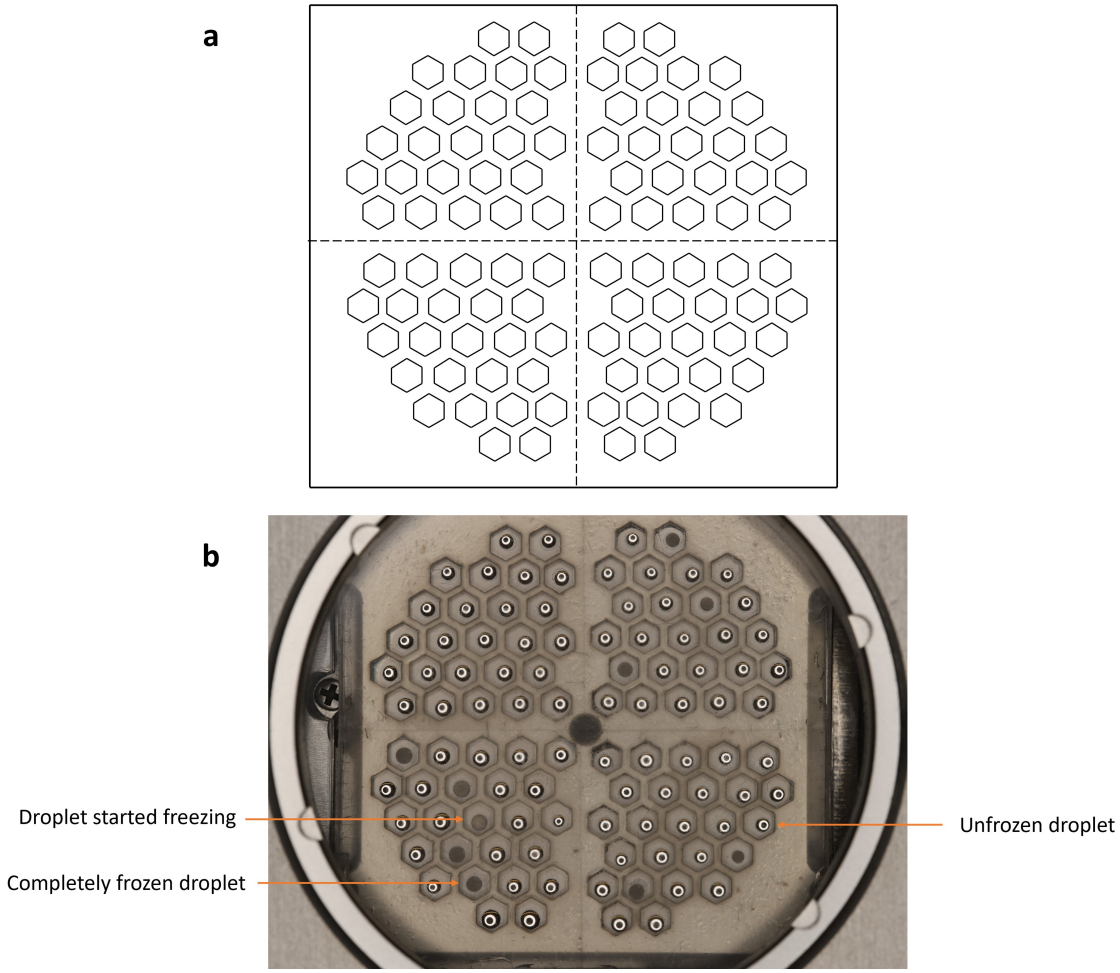

Figure 3.4: a) Pattern of the spacer that can be seen in Figure 3.3, that separate the droplets. The dashed lines shows how the hydrophobic glass slides are placed under the spacer as shown in Figure 3.3. b) A real photograph of the spacer which show the different freezing stages the sample droplets goes through on the cold stage.

The droplets will undergo a controlled freezing process. The different steps of the freezing process is called ramps. The temperature for the first ramp is at 23 °C while the droplets are being placed on the cold stage. After the placements of the drops N_2 gas is being used to help with trying to avoid condensation during the experiment. The second ramp will decrease the temperature from 23 °C to −5 °C. When this temperature is reached there is a minute wait time to let the droplets reach equilibrium before continuing to the third ramp. It is from this temperature (−5 °C) that the actual experiment begins and it is also at this transition from the second to third ramp the camera will start taking pictures. The third ramp takes the temperature from −5 °C to −38 °C (the cooling rate is 2 °C at this stage). The camera will take a picture every 5 seconds until all droplets are frozen and the experiment is stopped. The different stages of the sample droplets that can be seen during the freezing process on the cold stage can be seen in Figure 3.4b.

From the cold stage experiments hundreds of pictures are attained for each sample, like the one that can be seen in Figure 3.4b. Using image analysis the captured images are analyzed for the number of frozen droplets at given temperatures. The information is used for the equations in Chapter 4.1.

4

Data analysis

4.1 Deriving atmospheric INP concentrations

During the data analysis of the samples a few equations has been used. These equations have helped obtain the concentrations of INP from the analyzed samples. The data obtained from the cold stage measurements combined with Equations (4.1), (4.2) and (4.3) are the basis of the results presented in Chapter 5. Equation (4.1) will yield the frozen fraction (f_{ice}) which will show the percentage of the amount of drops that are frozen at a certain temperature.

$$f_{\text{ice}} = \frac{N_{\text{frozen}}(T)}{N_{\text{total}}}, \tag{4.1}$$

where f_{ice} is the frozen fraction, $N_{\text{frozen}}(T)$ is the number of drops that are frozen at temperature T and N_{total} is the total amount of drops, which is always 100 drops if all wells are filled.

Equation (4.2) will give the volume which is calculated as follows

$$V_{\text{air}} = \frac{V_{\text{sample}} \cdot f_{\text{fil}} \cdot V_{\text{drop}}}{V_{\text{wash}}} \tag{4.2}$$

where V_{air} $[m^3]$ is the volume of air, V_{sample} $[m^3]$ is the volume of the sampled air, f_{fil} is how big part of the filter that is used in the experiment (usually $\frac{1}{2}$ in these experiments), V_{drop} $[L]$ is the size of the drops placed on the cold stage (here 1 μL) and V_{wash} $[L]$ is the amount of purified water placed in the vials with the filter samples (here 2 ml).

Equation (4.3) will give the concentration of ice nucleating particles at a specific temperature.

$$N_{\text{INP}}(T) = \frac{-\ln(1 - f_{\text{ice}}(T))}{V} \tag{4.3}$$

where $N_{\mathrm{INP}}(T)$ $[m^{-3}]$ is the concentration of INP at a temperature T, f_{ice} is the frozen fraction at a temperature T and V $[m^3]$ is the volume.

4.2 Back trajectories

To help gain information about the correlation between INP concentrations and meteorological parameters back trajectories was used. Back trajectories help showcase from where the air masses have been travelling before reaching a specific destination which in this case is the Hyltemossa research station. An example of how these back trajectories can look like can be seen in Figure 4.1. Here the trajectory is 5 days long and on each day trajectories are calculated every 6 hours.

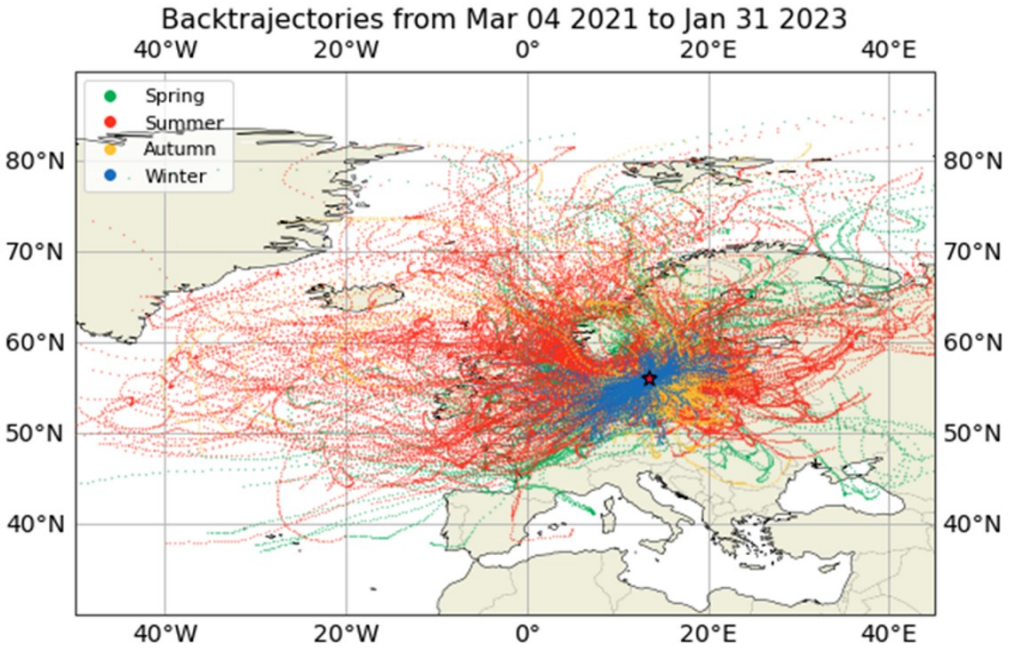

Figure 4.1: The back trajectory of the time period between March 2021 and January 2023. This trajectory is a 5 day long back trajectory and the air mass travels are divided into respective seasons. The dates used for the back trajectories are the one corresponding with the dates for the filter samples. There are no trajectories for dates between the middle of September 2021 to the middle of November 2022. On each day trajectories are calculated every 6 hours at 0:00, 6:00, etc. UTC and the height over Hyltemossa is set to 150 m.

To be able to do these back trajectories the Hybrid Single-Particle Lagrangian Integrated Trajectory (HYSPLIT) model is used. This model is one of the most used and will calculate an air masses path for a chosen time interval. [34] From these trajectories, information about if the air mass have spent most time over oceans or land can be gained.

5

Results and Discussion

5.1 Freezing spectra

Figure 5.1 shows the freezing spectra curves for the samples collected in August to September of 2021 and November 2022 to January 2023 and analyzed by me for this thesis project. It also shows the frozen fraction curve of a sample of pure MilliQ-water, where the MilliQ-water curve represent the background of LUCS. These samples are shown as a function of the freezing temperature ($°C$).

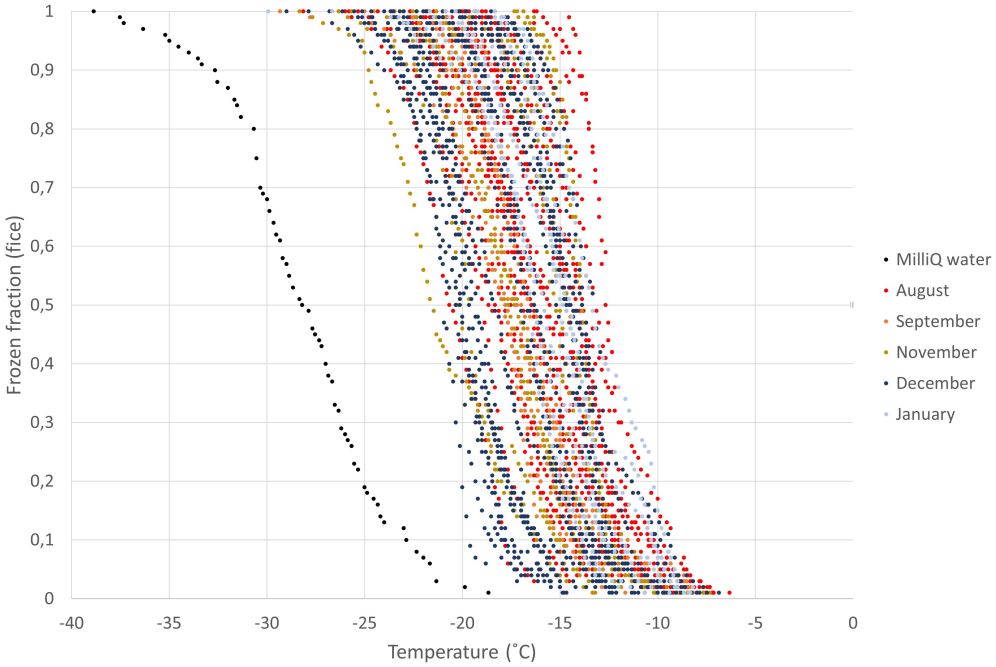

Figure 5.1: The frozen fraction of each sample collected between August-September 2021 and November-January 2022/2023 and of a sample of MilliQ-water as a function of the freezing temperature ($°C$).

From Figure 5.1 the freezing spectra of MilliQ-water is shown to have a freezing temperature range of −18 °C to −38 °C. The filter samples temperature range is instead between −7 °C and −30 °C. Since MilliQ-water is purified there should be very little to no contamination. So from this the conclusion can be drawn that there are ice nucleating particles present in the filter samples which will result in a higher freezing temperature. The curves for the samples also have the most data in the area of −15 °C which would indicate that around this temperature you would get the most range and information of the data set for other data analysis.

To further analyze the data from Figure 5.1 the data points are used to calculate each points corresponding INP concentration. With the calculated concentrations a time series were created, this can be seen in Chapter 5.2.

5.2 Time series of INP concentration

Figure 5.2 shows the time series for the INP concentration of filter samples seen in the freezing spectra in Figure 5.1 for the freezing temperatures −12 °C, −15 °C, −17 °C, −20 °C, −25 °C and −27 °C. To get a longer time series previously measured filter samples by Tamina Kabir, [35] are added to Figure 5.2 which results in the time series of INP concentrations seen in Figure 5.3. The same freezing temperatures are used for the longer time series as well. The shaded grey area in Figure 5.3 indicates the previously measured samples while the area without shading indicates the newly measured filters. The filters were collected from March to September 2021 and November 2022 to January 2023. Due to a change in the laboratory work an offset can be seen for these filter samples collected in 2022/2023.

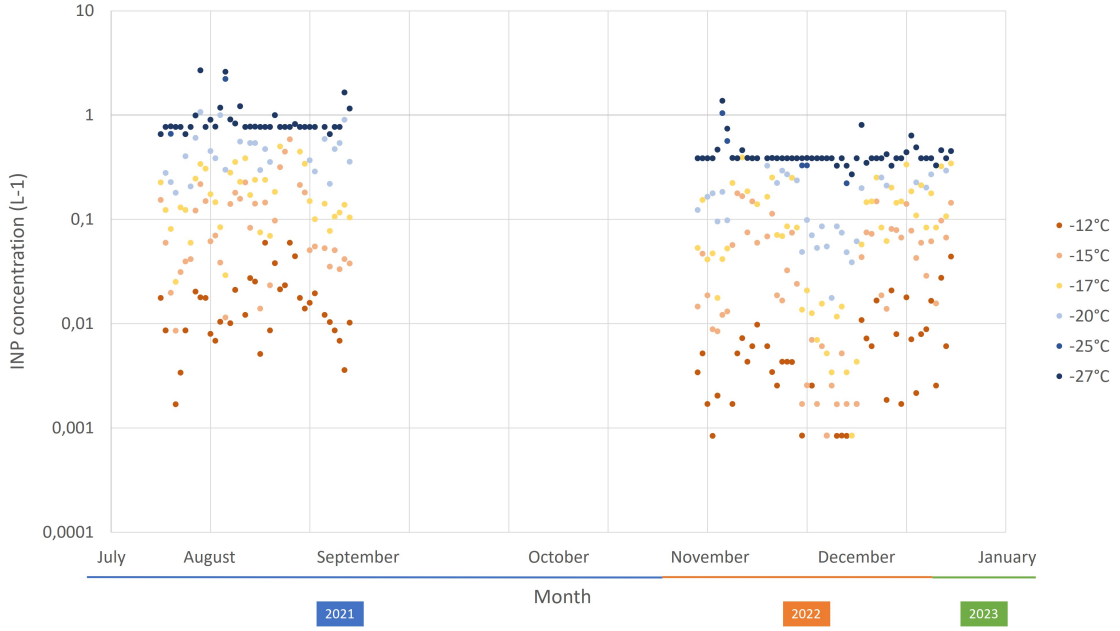

Figure 5.2: The time series with a logarithmic scale of INP concentrations from filter samples collected August to September 2021 and November 2022 to January 2023. The offset seen for the samples from 2022/2023 is due to a change in the laboratory process.

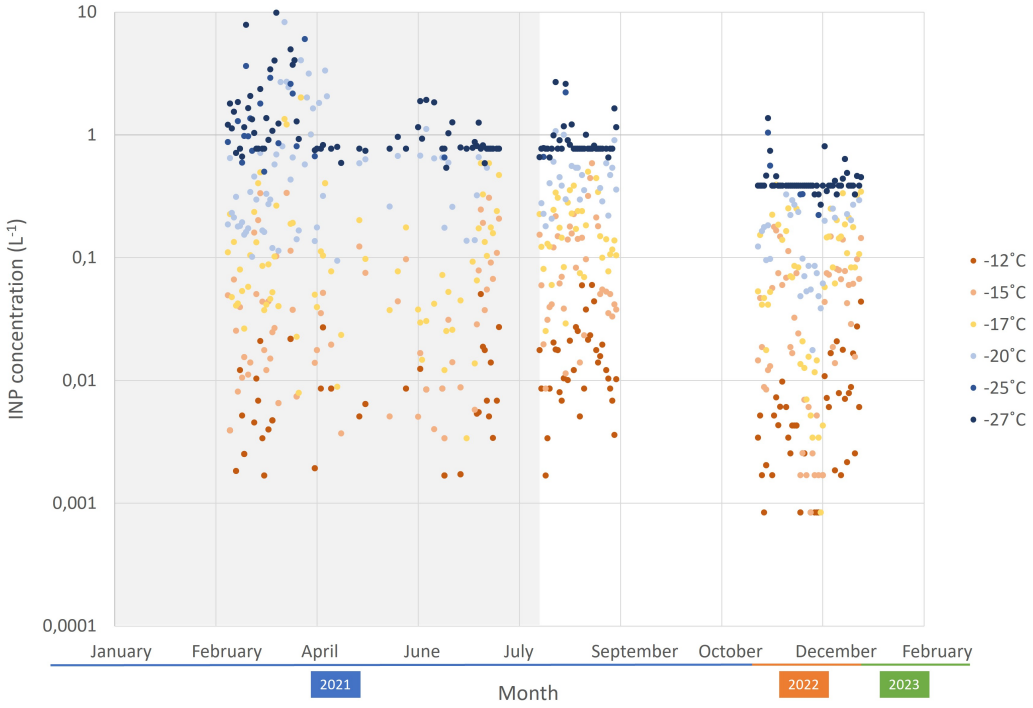

Figure 5.3: The time series with a logarithmic scale of INP concentrations from filter samples collected March to September 2021 and November 2022 to January 2023. The shaded grey area indicates the samples previously evaluated by Tamina Kabir, [35], and the area without shading are samples evaluated for this thesis. The offset seen for the samples from 2022/2023 is due to a change in the laboratory process.

When looking at the time series for previously measured samples and newly measured samples in Figure 5.3 there is not any big variability of the INP concentration that stands out. For all the samples from 2021 (March to September) the concentration is more or less constant for the different freezing temperatures that have been chosen. When it comes to the samples collected 2022/2023 (November to January) the offset that can be seen is due to a change in the laboratory routine. All samples for the 2021 period have used half of the filter while the samples for the 2022/2023 period has used the whole filter. When calculating the concentration of INP, Equation 4.3 is used. To be able to use this you first need to calculate the volume of air with Equation 4.2, where the amount of filter used in the experiment is needed. When using half a filter you only account for half the sampled air volume which can be seen in Equation 4.2. This will change the range of the measurable concentration and thus gives this type of offset when close to the lower limit of detection. If this offset is disregarded there doesn't seem to be any seasonal variability that stands out. This can also be seen in Table 5.1 where the average INP concentrations at different temperatures for each month is shown. Here the average INP concentration is shown to only have slight variability between the different months.

Table 5.1: The average INP concentration (L^{-1}) for each month of the time series in Figure 5.3.

	Average INP concentration (L^{-1}) at T=-12°C	Average INP concentration (L^{-1}) at T=-15°C	Average INP concentration (L^{-1}) at T=-17°C	Average INP concentration (L^{-1}) at T=-20°C	Average INP concentration (L^{-1}) at T=-25°C	Average INP concentration (L^{-1}) at T=-27°C
March (2021)	0.00264	0.05225	0.17729	0.80391	0.96449	1.97746
April (2021)	0.00308	0.01363	0.28421	1.08436	1.41815	3.02706
May (2021)	0.00402	0.06877	0.11777	0.58386	0.80171	0.80171
June (2021)	0.00253	0.00769	0.03714	0.64930	1.10089	1.10979
July (2021)	0.01340	0.11862	0.25246	0.64022	0.81105	0.81105
August (2021)	0.01691	0.15943	0.26510	0.60722	0.92595	0.94289
September (2021)	0.01087	0.04449	0.11638	0.46603	0.91251	0.91251
November (2022)	0.00365	0.06192	0.16261	0.27783	0.46104	0.49989
December (2022)	0.00437	0.03988	0.09485	0.22675	0.39207	0.39943
January (2023)	0.01441	0.06444	0.17946	0.32672	0.40871	0.40871

The time series of the INP concentrations do not seem to show any variability between different months and seasons and neither does the average INP concentrations. To see if there is a correlation between the INP concentrations of the filter samples and meteorological and aerosol parameters an analysis was made, see Chapter 5.3.

5.3 Correlations

Figure 5.4 shows a heatmap where the correlation between INP concentrations, meteorological parameters and aerosol properties can be seen. To see the individual plotted meteorological and aerosol property data for the sample period see Appendix A. The meteorological data for the wind speed, temperature, precipitation and photosynthetic photon flux density (PPFD) are measured at Hyltemossa research station by ICOS [28]. The PM data is measured by Naturvårdsverket in Hallahus which is located $\approx 15\,\text{km}$ from Hyltemossa. The biological particles are measured at Hyltemossa research station by ACTRIS [29].

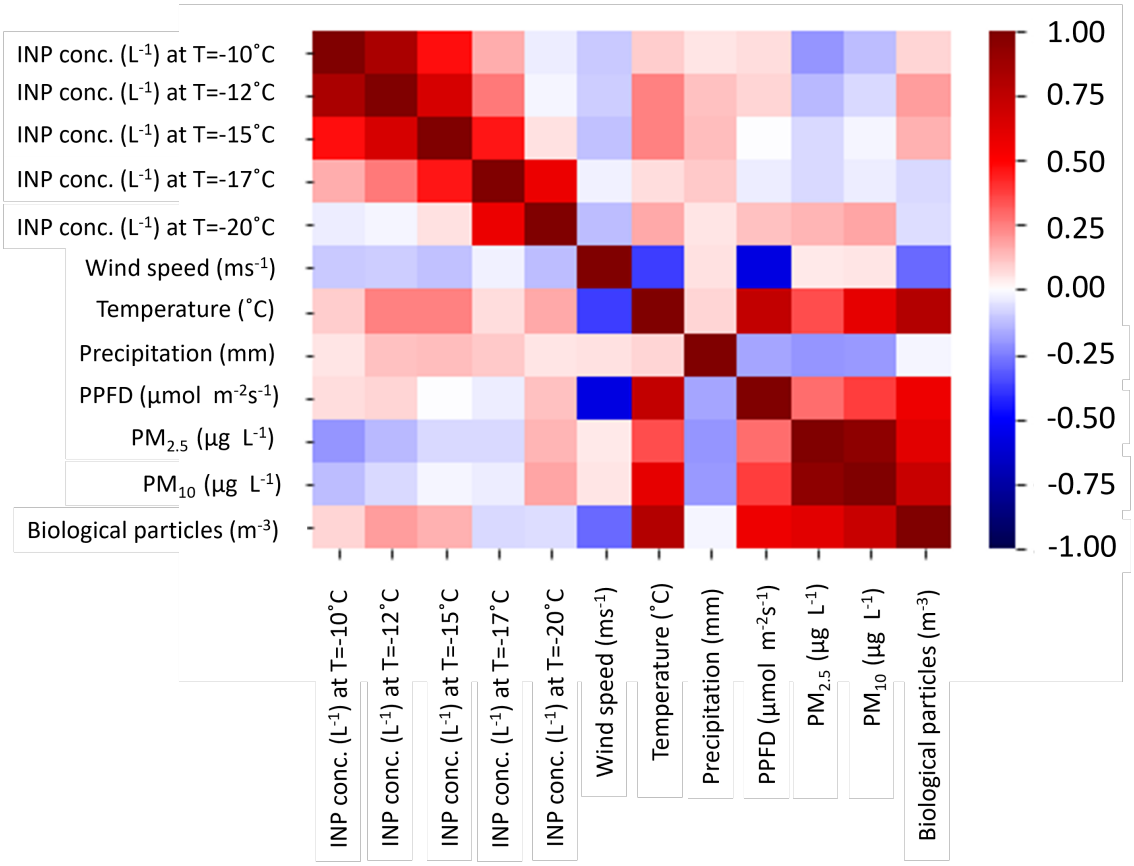

Figure 5.4: A heatmap showing the correlations between the INP concentration for the temperatures $-10°C$, $-12°C$, $-15°C$, $-17°C$ and $-20°C$ and meteorological parameters (wind speed (ms^{-1}), temperature ($°C$), precipitation (mm) and photosynthetic photon flux density ($\mu \text{mol} m^{-2} s^{-1}$) and aerosol mass concentrations ($PM_{2.5}$ ($\mu g L^{-1}$), PM_{10} ($\mu g L^{-1}$) and concentration of biological particles (m^{-3}). The colour bar in the heatmap show the correlations of two parameters. The positive numbers (red part of colour bar) indicates a correlation between the parameters. The negative numbers (blue part) indicates there is not a correlation between the parameters.

Table 5.2 shows the calculated Spearman's rank correlation coefficient and p-value for the correlations between INP concentration and meteorological parameters and aerosol properties.

Table 5.2: The calculated Spearman's rank correlation coefficient (ρ) and p-value for the different meteorological parameters and aerosol properties from Figure 5.4. Where p-values < 0.05 are statistically significant and marked yellow in the table.

	INP concentration at T=-10°C		INP concentration at T=-12°C		INP concentration at T=-15°C		INP concentration at T=-17°C		INP concentration at T=-20°C	
	ρ	p -value	ρ	p - value	ρ	p - value	ρ	p - value	ρ	p - value
Wind speed	-0,02324	0,78366	-0,06691	0,42883	-0,07897	0,35018	-0,06353	0,45256	-0,27257	0,00103
Temperature	0,16109	0,05546	0,19839	0,01794	0,24299	0,00357	0,25287	0,00239	0,56869	1,548e-13
Precipitation	0,23077	0,00572	0,16888	0,04453	0,12384	0,14201	0,18969	0,02376	0,05682	0,50178
PPFD	-0,08616	0,30795	-0,04606	0,58623	-0,05038	0,55154	-0,06259	0,45924	0,40347	6,4e-07
$PM_{2.5}$	-0,21422	0,07496	-0,24265	0,04298	-0,18009	0,13575	-0,13526	0,26422	0,17324	0,15152
PM_{10}	-0,08354	0,49174	-0,08794	0,46913	-0,07069	0,56089	-0,06811	0,57529	0,17618	0,14459
Biological particles	0,26469	0,00345	0,34615	0,00011	0,30039	0,00086	0,15915	0,08251	0,20384	0,02554

For more comparisons of aerosol properties and meteorological parameters to INP concentrations some correlation coefficients have been calculated. Firstly, a look at Figure 5.4 shows some things that would be expected when looking at correlations. For example there is an indication that biological particles and temperature have a quite strong correlation. This is intuitively something that seems right since there will be more biological particles, such as pollen, when the temperature is starting to rise. Secondly, another correlation that can be seen is between temperature and photosynthetic photon flux density (PPFD) and also between biological particles and PPFD. A negative correlation can also be found between PPFD and precipitation, this is probably due to the fact that when there is precipitation it will also be cloudy which interfere with PPFD. When looking at the INP concentrations and there correlations to meteorological parameters and aerosol properties it is easier to look at Table 5.2. In this table the Spearman's rank correlation coefficient has been calculated and also the p-value. The reason for using the Spearman's rank correlation instead of the Pearson correlation is due to the fact that Spearman evaluates monotonic relationships of the parameters. This means that the correlation between two parameters do not need to have a linear relationship to be shown to have a high correlation coefficient unlike the Pearson correlation. The highlighted p-values indicates that there is something that is statically significant. From Table 5.2 the biological particles and temperatures gives some indication that there could

be something statistically significant there. From the Spearman coefficient (ρ) there isn't a big indication that the concentration of INP and the temperature and biological particles have a strong correlation. To be able to determine this with more certainty a longer time series, of several years, would have to be done in order to find the average season of a year. With a smaller time series, like this, that is less then a year an unusual weather event could lead to drawing the wrong conclusions.

To look a bit closer to the weak correlation between INP concentrations and biological particles an analysis of measured pollen and INP concentration was done as well. This analysis is seen in Chapter 5.4.

5.4 Pollen

Figure 5.5 a) shows the pollen count that has been measured in Hässleholm by pollenkollen [36]. Hässleholm is the closest pollen measuring site to Hyltemossa research station and both of their locations can be seen in Figure 3.1. The distance between Hässleholm and Hyltemossa is $\approx 23\,\text{km}$. The plot has been altered by translating the Swedish word to English and by adding the blue and red square to the plot. The time period is between January 2021 and June 2021, alder is blue, birch is red and oak is yellow. The squares in the plot is corresponding to the time period shown in Figure 5.5 b). Figure 5.5 b) shows the INP concentration for the time period March 2021 to May 2021 for the temperatures $-12\,^{\circ}\text{C}$, $-15\,^{\circ}\text{C}$ and $-17\,^{\circ}\text{C}$.

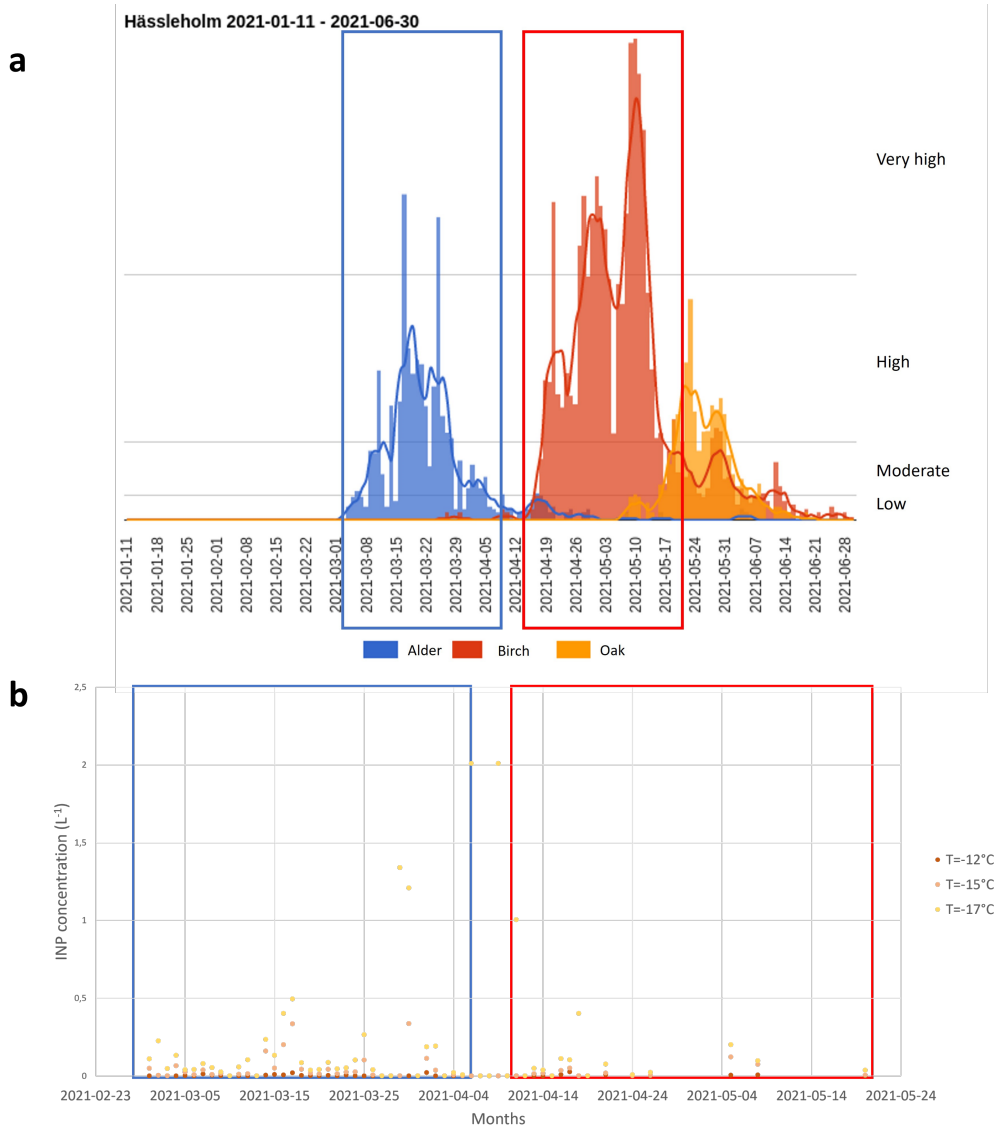

Figure 5.5: a) shows the amount of pollen from the Hässleholm region ($\approx$ 23 km from Hyltemossa) in the time period of January 2021 to June 2021 [36]. Where alder is blue, birch is red and oak is yellow. (This plot has been altered in power point by changing the names from Swedish to English and the adding of the squares) b) shows the INP concentration measured from the filter samples for the time period March 2021 to May 2021 for the temperatures $-12\,°C$, $-15\,°C$ and $-17\,°C$. The blue and red square in the plot correspond to the same time period as shown in a). Figure a) adapted from [36].

Figure 5.6 a) shows the pollen count that has been measured in Hässleholm by pollenkollen [36]. Hässleholm is the closest pollen measuring site to Hyltemossa research station and both of their locations can be seen in Figure 3.1. The distance between Hässleholm and Hyltemossa is ≈ 23 km. (The plot has been altered by translating the Swedish word to English and by adding the yellow square to the plot). The time period is between May 2021 and September 2021, ambrosia artemisiifolia is blue, artemisia vulgaris is red and grass is yellow. The squares in the plot is corresponding to the time period shown in Figure 5.6 b). Figure 5.6 b) shows the INP concentration for the time period May 2021 to July 2021.

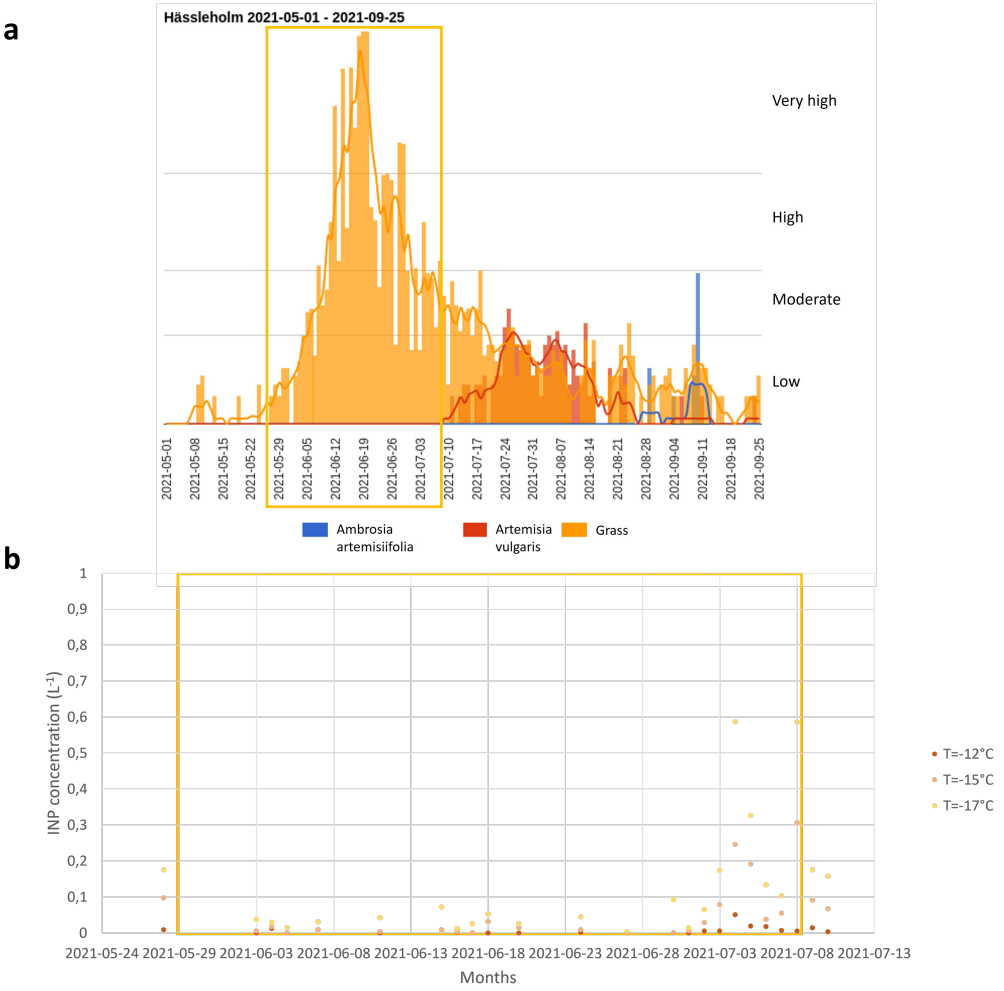

Figure 5.6: a) shows the amount of pollen from the Hässleholm region (≈ 23 km from Hyltemossa) in the time period of May 2021 to September 2021 [36]. Where ambrosia artemisiifolia is blue, artemisia vulgaris is red and grass is yellow. (This plot has been altered in power point by changing the names from Swedish to English and the adding of the squares) b) shows the INP concentration measured from the filter samples for the time period May 2021 to July 2021 for the temperatures −12 °C, −15 °C and −17 °C. The yellow square in the plot correspond to the same time period as shown in a). Figure a) adapted from [36].

From Figure 2.5 pollen shows to be INP active at temperatures of −20 °C and above. For a further look at this, INP concentrations at −12 °C, −15 °C and −17 °C were compared to pollen measured as seen in Figure 5.5 and Figure 5.6. The reason for choosing these temperatures was due to the fact that pollen is known to be better INPs at higher temperatures [21]. From the pollen comparison there are not any peaks in INP concentrations that corresponds to the peaks of the pollen counts. This is not suprising since the Spearman's rank correlation coefficients and p-values for the biological particles are quite low.

Previous investigations of pollutants have shown that the measured concentrations will show a frequency distribution that is behaving lognormal or close to lognormal if the samples are well mixed [37]. To investigate if the air masses for the analyzed filter samples are well mixed a frequency distribution for the INP concentrations were done, see Chapter 5.5.

5.5 Frequency distribution

Figure 5.7 shows the frequency distribution of measured INP concentrations for different freezing temperatures. Here the measured INP concentrations are shown in a histogram with an added Gaussian fit.

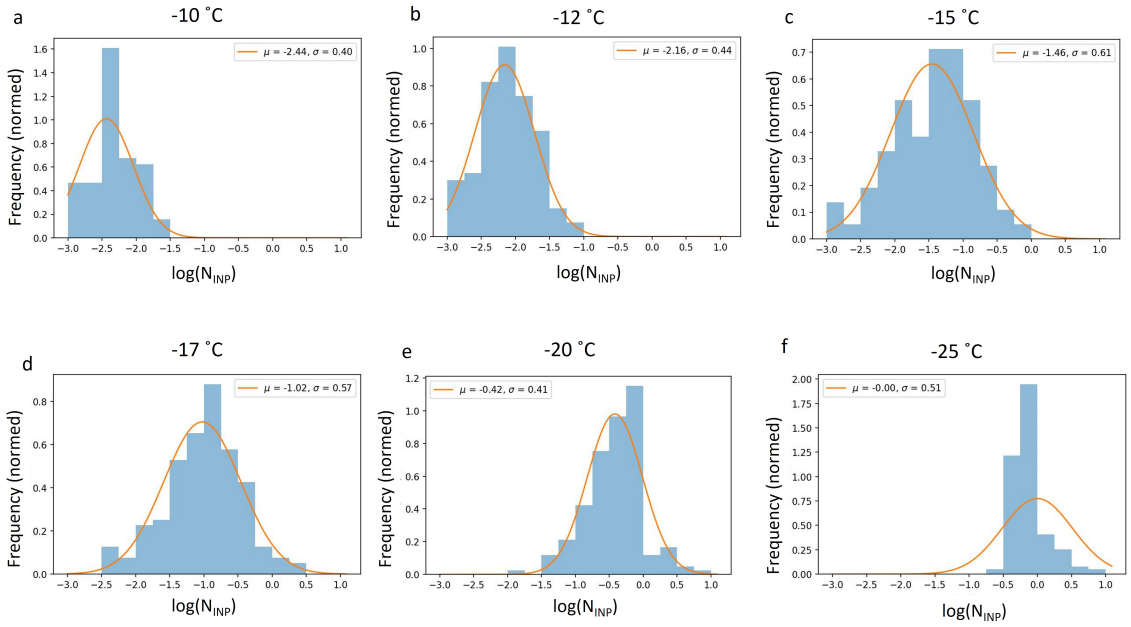

Figure 5.7: The frequency distribution of measured INP concentrations for different freezing temperatures. A Gaussian fit has also been added. The selected freezing temperatures shown are: a) −10 °C, b) −12 °C, c) −15 °C, d) −17 °C, e) −20 °C, f) −25 °C.

Measured concentrations of pollutants will show a lognormal frequency distribution if the samples are well mixed, this has been shown in investigations like Ott (1990) [37]. Air masses that has been travelling long distances will have had more time to go through additional mixing. To examine this phenomenon on my samples a frequency distribution was plotted with my measured INP concentrations. As can be seen in Figure 5.7 some of the frequency distributions have a lognormal behaviour. Figure 5.7 shows that the logarithms of the INP concentrations most alike a lognormal distribution for the sampled filters are at $-15\,^{\circ}\mathrm{C}$ and $-17\,^{\circ}\mathrm{C}$. This gives an indication that these air masses have been well mixed and had traveled a longer distance before they have been sampled. From this the conclusion can be drawn that the air mass arriving did not encounter any local sources of ice nucleating particles. Which also is what was observed with previous Figures from Chapter 5.4. A deviation from log-normaility indicate the contribution of either local sources or very clean air masses to the measured INP population. A reason for deviation from lognormal distribution for the lowest freezing temperatures are due to that the counting limit has been reached at this point. It means that the concentrations of INPs at this point is very high and everything has been frozen and you have basically hit the limit of the experimental resolution.

Since Figure 5.7 indicates that the air masses are well mixed an interesting question to investigate is where the air masses come from before reaching Hyltemossa research station. This has been done in Chapter 5.6.

5.6 Back trajectories

Figure 5.8 shows 5 day long back trajectories for the time period of March to September 2021 and November 2022 to January 2023. The trajectories have been divided into the different seasons of the year where spring is green, summer is red, autumn is yellow and winter is blue. Where the height over Hyltemossa was set to 150 m and the trajectories for each day was calculated every 6 hours at 0:00, 6:00, etc UTC.

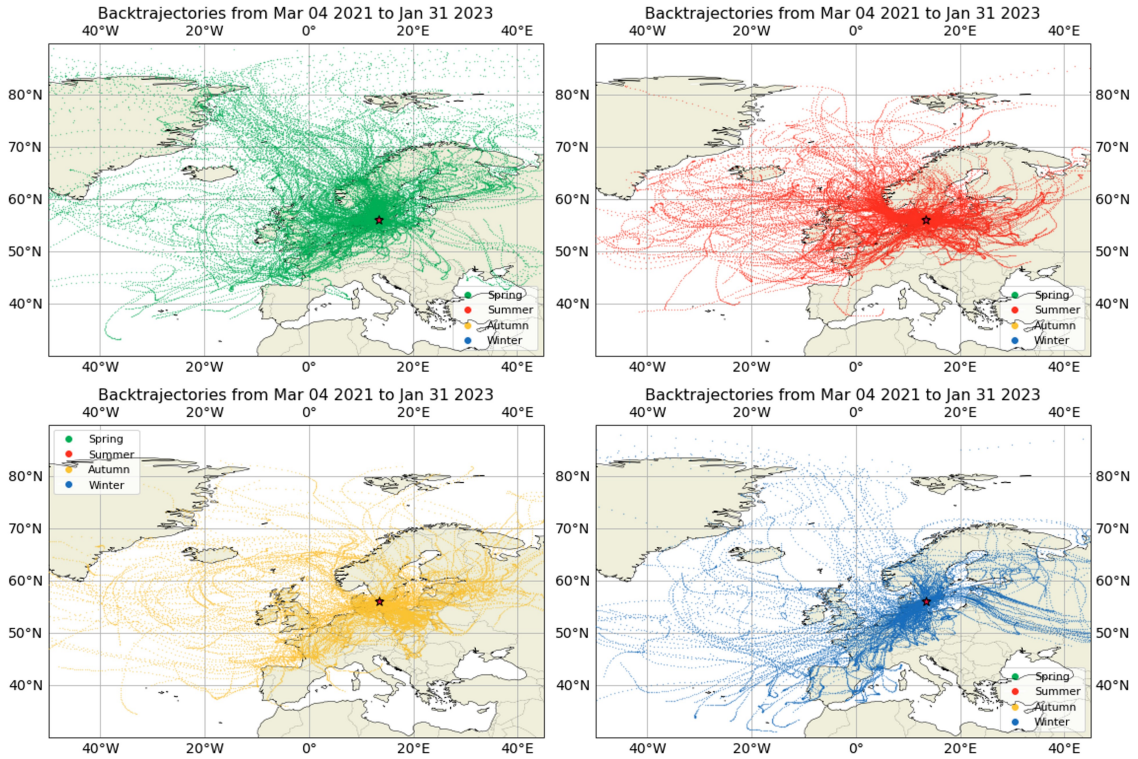

Figure 5.8: Back trajectories for the whole time period of March to September 2021 and November 2022 to January 2023. Where they have been divided into the different seasons of the year, where spring is green, summer is red, autumn is yellow and winter is blue. The trajectory is 5 days long, the height over Hyltemossa was set to 150 m and the trajectories for each day was calculated every 6 hours at 0:00, 6:00, etc UTC.

Figure 5.9 and Figure 5.10 shows a 10 day back trajectory for the day with the highest respective lowest freezing temperature for the months of August (2021), September (2021), November (2022), December (2022) and January (2023). The plots for determining these days can be found in Appendix B

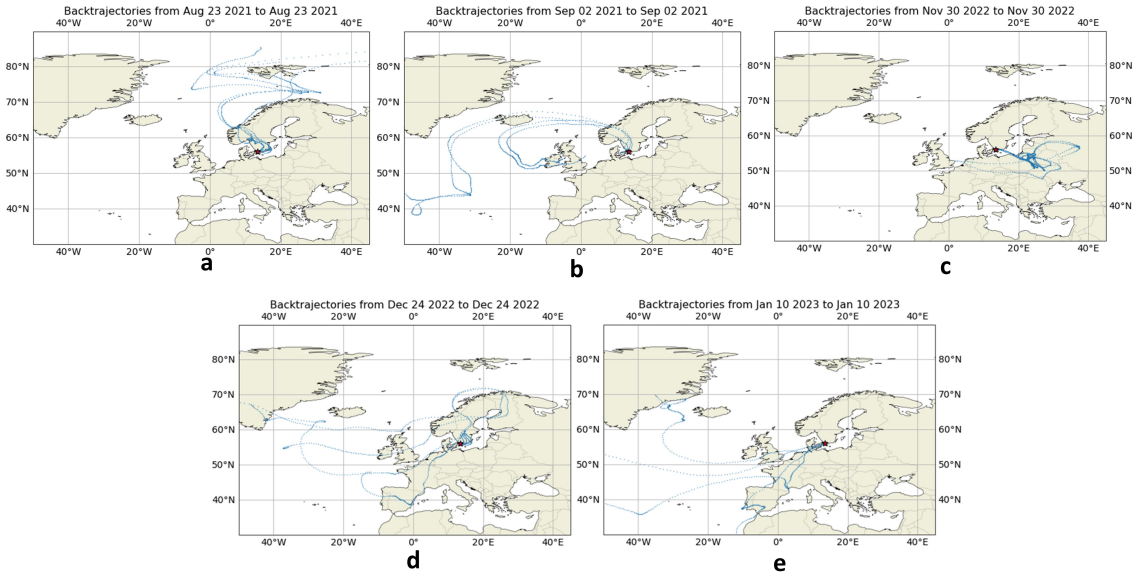

Figure 5.9: Back trajectories for the highest freezing temperature for each month of a) August (2021), b) September (2021), c) November (2022), d) December (2022) and e) January (2023). All trajectories shown are 10 days long.

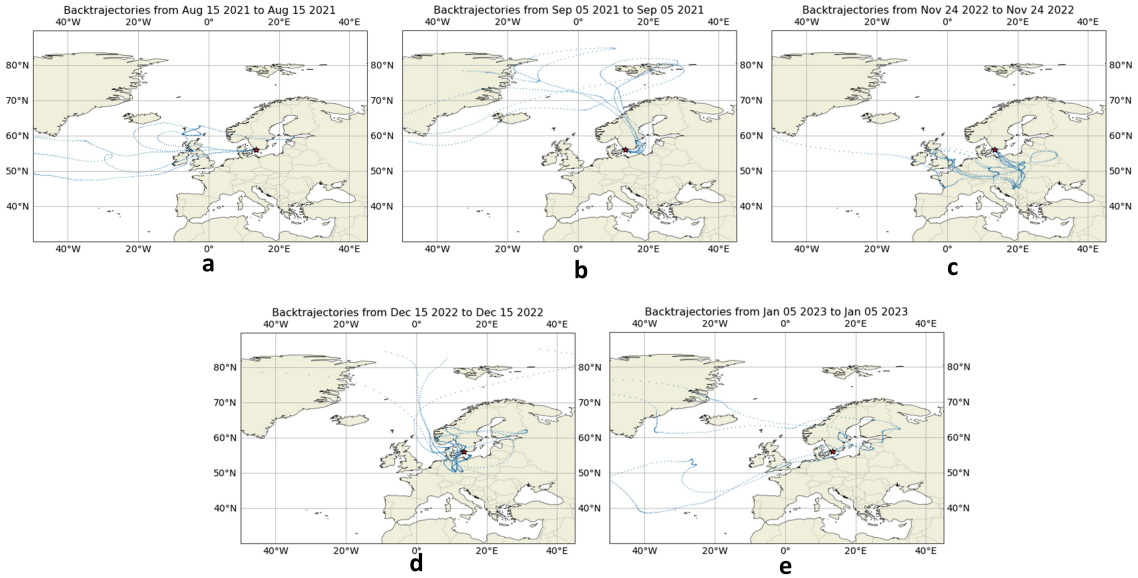

Figure 5.10: Back trajectories for the lowest freezing temperature for each month of a) August (2021), b) September (2021), c) November (2022), d) December (2022) and e) January (2023). All trajectories shown are 10 days long.

For back trajectories in Figure 5.8 there doesn't seem to be a correlation between the time of year and how the air mass have traveled. This is something that, when comparing to Figure 5.3, seem to be accurate. Since there isn't any major deviations in the concentrations of the ice nucleating particles during the time period the assumption would be that the air mass would have similar travel patterns during the dates of the evaluated filter samples.

Back trajectories for the highest and lowest INP concentration days in Figure 5.9 respectively Figure 5.10 indicates that the travel pattern of the air masses isn't an indication if there will be a higher or lower measured INP concentration. Most of the days for both the high and low cases have air masses that have traveled over the Atlantic ocean before reaching Hyltemossa.

Another interesting question is to see how the measured filter samples compares to other collected sample data. To see how my INP concentration data compares with other INP concentration data two different parametrizations have been used. These parametrizations are DeMott et al. (2010) and Schneider et al. (2021) and can be seen in Chapter 5.7.

5.7 Parametrization

Different parametrizations have been developed to help with predicting INP concentrtaions and to achieve more accurate climate models. Two of these parametrizations are used here to compare with the evaluated filter samples. The first one is DeMott et al. (2010) parametrization and it is as follows [38]

$$N_{\mathrm{INP}}(T_{\mathrm{k}}) = a(273.16 - T_{\mathrm{k}})^{b}(n_{\mathrm{aer},0.5})^{(c(273.16-T_{\mathrm{k}})+d)} \tag{5.1}$$

where $a = 0.0000594$, $b = 3.33$, $c = 0.0264$, $d = 0.0033$, T_{k} is the temperature of the cloud in Kelvin, $n_{\mathrm{aer},0.5}$ is the aerosol particle number concentration of particles that are larger than $0.5\mu m$ in scm^{-3} and $N_{\mathrm{INP}}(T_{\mathrm{k}})$ is the INP number concentration in $stdL^{-1}$ at a specific temperature T_{k}.

The other parametrization used is the Schneider et al. (2021) and it is as follows [39]

$$N_{\mathrm{INP}} = 0.1 \cdot exp(a1 \cdot T_{\mathrm{amb}} + a2) \cdot exp(b1 \cdot T + b2) \tag{5.2}$$

where $a1 = 0.074 \pm 0.006 K^{-1}$, $a2 = -18 \pm 2$, $b1 = -0.504 \pm 0.005 K^{-1}$. $b2 = 127 \pm 1$, T is the activation temperature in Kelvin, T_{amb} is the ambient air temperature in Kelvin and N_{INP} is the concentration of INP in $stdL^{-1}$

Figure 5.11 shows the filter samples evaluated for this thesis in colour (August - January) and previously evaluated filter samples. by Tamina Kabir, in grey [35]. The parametrizations from DeMott et al. (2010) and Schneider et al. (2021) is also added to this plot.

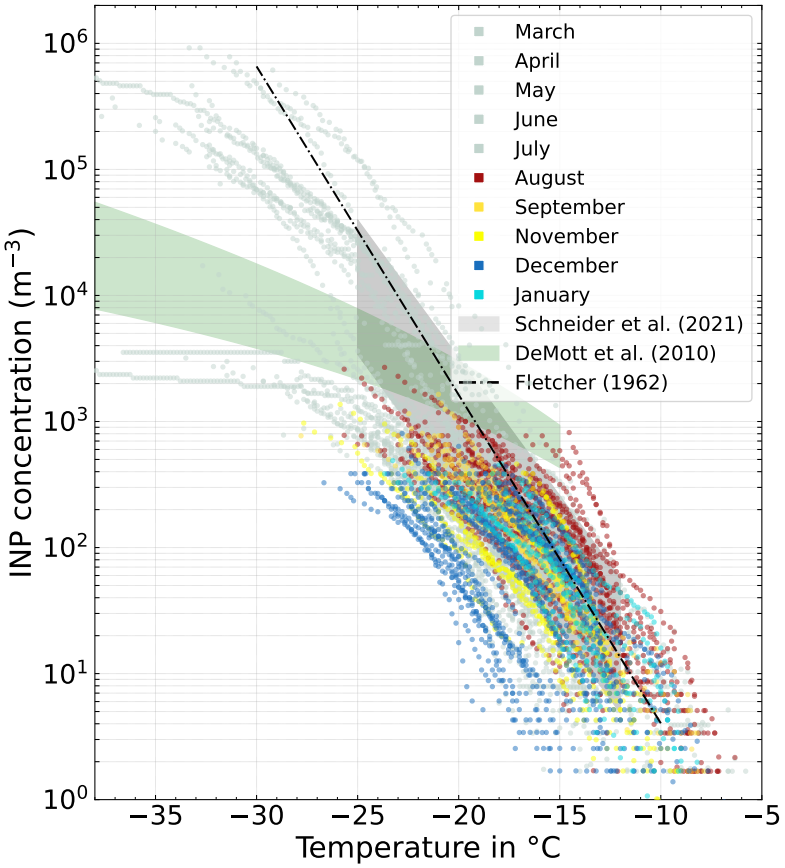

Figure 5.11: The INP concentration (m^{-3}) at their freezing temperature ($°C$). The INP concentration samples in colour were evaluated for this thesis while the INP concentrations samples in grey were previously evaluated by Tamina Kabir, [35]. For this plot the parametrizations developed by DeMott et al. (2010) [38] and Schneider et al. (2021) [39] are added. The DeMott et al. (2010) parametrization was developed for temperatures lower than $-15°C$ while the Schneider et al. (2021) was developed for temperatures between $-12°C$ and $-25°C$.

The parametrization developed by DeMott et al. (2010) seems to be overestimate the INP concentrations. The parametrization was developed for temperatures below −15 °C. They also based it on several regions around the world and with a data set with a time period of about 14 years. Since the time period here is less than a year it could indicate that if more data were collected it could start matching the DeMott et al. (2010) parametrization. Since the used regions for the DeMott et al. (2010) were collected from around the world while the filter samples were all from one region it could also be the reason for the bad fit.
The Schneider et al. (2021) parametrization was based on over a year long data set from a boreal forest in Hyytiäla, Finland. The temperature range which it was developed was between −12 °C and −25 °C. For this parametrization the data set matches better than for the DeMott et al. (2021) parametrization. There is in this case like the other an overestimation of the INP concentration. For the Schneider et

al. (2021) parametrization they could see a seasonal variation which isn't the case for my results. A reson for this could be the region difference. For the Hyltemossa research station site there isn't a long period of time where there is snow coverage. There is also less variation in temperature here compared to the Hyytiäla region. When there is snow coverage a longer time the biological particles might have a burst when spring arrives and the snow coverage disappears. This could give the effect of a seasonal variability. It could also be due to the fact that the time series for this thesis isn't even a year long.

6

Conclusion

From the results gained from this study there are some conclusions that can be drawn. From looking at the concentration of ice nucleating particles during the time period no trends could be seen seasonally. It indicates that air masses that reach Hyltemossa research station are well mixed and not affected by any local sources.

For the correlation between INP concentration and meteorological parameters and aerosol particles there seem to be a weak correlation regarding the INP concentration with temperature and biological particles. But in regards to the biological particles no correlation could be found in comparison between measured INP concentrations and measured pollen counts.

How air masses travels before reaching a region does not seem to give an indication of expected INP concentration. There could instead be other variables that determines INP concentrations.

To be able to have a more definitive answer more data need to be collected to get a longer time series. With a longer time series more seasonal patterns may emerge which could in turn lead to being able to see an influence from it on the INP concentration.

Bibliography

[1] S. Szopa, V. Naik, B. Adhikary, P. Artaxo, T. Berntsen, W.D. Collins, S. Fuzzi, L. Gallardo, A. Kiendler-Scharr, Z. Klimont, H. Liao, N. Unger, and P. Zanis. , 2021:Short-Lived Climate Forcers. In Climate Change 2021: The Physical Science Basis. Contribution of Working Group I to the Sixth Assessment Report of the Intergovernmental Panel on Climate Change. In V. Masson-Delmotte, P. Zhai, A. Pirani, S.L. Connors, C. Péan, S. Berger, N. Caud, Y. Chen, L. Goldfarb, M.I. Gomis, M. Huang, K. Leitzell, E. Lonnoy, J.B.R. Matthews, T.K. Maycock, T. Waterfield, O. Yelekçi, R. Yu, and B. Zhou, editors, *IPCC 2021*, pages 817–922. Cambridge University Press, Cambridge, United Kingdom and New York, NY, USA, 2021.

[2] Z. Brasseur, D. Castarède, E. S. Thomson, M. P. Adams, S. Drossaart van Dusseldorp, P. Heikkilä, K. Korhonen, J. Lampilahti, M. Paramonov, J. Schneider, F. Vogel, Y. Wu, J. P. D. Abbatt, N. S. Atanasova, D. H. Bamford, B. Bertozzi, M. Boyer, D. Brus, M. I. Daily, R. Fösig, E. Gute, A. D. Harrison, P. Hietala, K. Höhler, Z. A. Kanji, J. Keskinen, L. Lacher, M. Lampimäki, J. Levula, A. Manninen, J. Nadolny, M. Peltola, G. C. E. Porter, P. Poutanen, U. Proske, T. Schorr, N. Silas Umo, J. Stenszky, A. Virtanen, D. Moisseev, M. Kulmala, B. J. Murray, T. Petäjä, O. Möhler, and J. Duplissy. Measurement report: Introduction to the hyice-2018 campaign for measurements of ice-nucleating particles and instrument inter-comparison in the hyytiälä boreal forest. *Atmospheric Chemistry and Physics*, 22(8):5117–5145, 2022.

[3] J. Schneider, K. Höhler, P. Heikkilä, J. Keskinen, B. Bertozzi, P. Bogert, T. Schorr, N. S. Umo, F. Vogel, Z. Brasseur, Y. Wu, S. Hakala, J. Duplissy, D. Moisseev, M. Kulmala, M. P. Adams, B. J. Murray, K. Korhonen, L. Hao, E. S. Thomson, D. Castarède, T. Leisner, T. Petäjä, and O. Möhler. The seasonal cycle of ice-nucleating particles linked to the abundance of biogenic aerosol in boreal forests. *Atmospheric Chemistry and Physics*, 21(5):3899–3918, 2021.

[4] D. O'Sullivan, B. J. Murray, T. L. Malkin, T. F. Whale, N. S. Umo, J. D. Atkinson, H. C. Price, K. J. Baustian, J. Browse, and M. E. Webb. Ice nucleation by fertile soil dusts: relative importance of mineral and biogenic components. *Atmospheric Chemistry and Physics*, 14(4):1853–1867, 2014.

[5] H. Wex, L. Huang, W. Zhang, H. Hung, R. Traversi, S. Becagli, R. J. Sheesley, C. E. Moffett, T. E. Barrett, R. Bossi, H. Skov, A. Hünerbein, J. Lubitz,

M. Löffler, O. Linke, M. Hartmann, P. Herenz, and F. Stratmann. Annual variability of ice-nucleating particle concentrations at different arctic locations. *Atmospheric Chemistry and Physics*, 19(7):5293–5311, 2019.

[6] C. Budke and T. Koop. Binary: an optical freezing array for assessing temperature and time dependence of heterogeneous ice nucleation. *Atmospheric Measurement Techniques*, 8(2):689–703, 2015.

[7] D. Chen, M. Rojas, B.H. Samset, K. Cobb, A. Diongue Niang, P. Edwards, S. Emori, S.H. Faria, E. Hawkins, P. Hope, P. Huybrechts, M. Meinshausen, S.K. Mustafa, G.-K. Plattner, and A.-M. Tréguier. , 2021:Framing, Context, and Methods. In Climate Change 2021: The Physical Science Basis. Contribution of Working Group I to the Sixth Assessment Report of the Intergovernmental Panel on Climate Change. In V. Masson-Delmotte, P. Zhai, A. Pirani, S.L. Connors, C. Péan, S. Berger, N. Caud, Y. Chen, L. Goldfarb, M.I. Gomis, M. Huang, K. Leitzell, E. Lonnoy, J.B.R. Matthews, T.K. Maycock, T. Waterfield, O. Yelekçi, R. Yu, and B. Zhou, editors, *IPCC 2021*, pages 147–286. Cambridge University Press, Cambridge, United Kingdom and New York, NY, USA, 2021.

[8] P.A. Arias, N. Bellouin, E. Coppola, R.G. Jones, G. Krinner, J. Marotzke, V. Naik, M.D. Palmer, G.-K. Plattner, J. Rogelj, M. Rojas, J. Sillmann, T. Storelvmo, P.W. Thorne, B. Trewin, K. Achuta Rao, B. Adhikary, R.P. Allan, K. Armour, G. Bala, R. Barimalala, S. Berger, J.G. Canadell, C. Cassou, A. Cherchi, W. Collins, W.D. Collins, S.L. Connors, S. Corti, F. Cruz, F.J. Dentener, C. Dereczynski, A. Di Luca, A. Diongue Niang, F.J. Doblas-Reyes, A. Dosio, H. Douville, F. Engelbrecht, V. Eyring, E. Fischer, P. Forster, B. Fox-Kemper, J.S. Fuglestvedt, J.C. Fyfe, N.P. Gillett, L. Goldfarb, I. Gorodetskaya, J.M. Gutierrez, R. Hamdi, E. Hawkins, H.T. Hewitt, P. Hope, A.S. Islam, C. Jones, D.S. Kaufman, R.E. Kopp, Y. Kosaka, J. Kossin, S. Krakovska, J.-Y. Lee, J. Li, T. Mauritsen, T.K. Maycock, M. Meinshausen, S.-K. Min, P.M.S. Monteiro, T. Ngo-Duc, F. Otto, I. Pinto, A. Pirani, K. Raghavan, R. Ranasinghe, A.C. Ruane, L. Ruiz, J.-B. Sallée, B.H. Samset, S. Sathyendranath, S.I. Seneviratne, A.A. Sörensson, S. Szopa, I. Takayabu, A.-M. Tréguier, B. van den Hurk, R. Vautard, K. von Schuckmann, S. Zaehle, X. Zhang, and K. Zickfeld. , 2021: Technical Summary. In Climate Change 2021: The Physical Science Basis. Contribution of Working Group I to the Sixth Assessment Report of the Intergovernmental Panel on Climate Change. In V. Masson-Delmotte, P. Zhai, A. Pirani, S.L. Connors, C. Péan, S. Berger, N. Caud, Y. Chen, L. Goldfarb, M.I. Gomis, M. Huang, K. Leitzell, E. Lonnoy, J.B.R. Matthews, T.K. Maycock, T. Waterfield, O. Yelekçi, R. Yu, and B. Zhou, editors, *IPCC 2021*, pages 33–144. Cambridge University Press, Cambridge, United Kingdom and New York, NY, USA, 2021.

[9] G. Myhre, C. Lund Myhre, B. H. Samset, and T. Storelvmo. Aerosols and their relation to global climate and climate sensitivity. *Nature Education Knowledge*, 4:7, 05 2013.

[10] R. Johansson. Measurements of atmospheric ice nucleating particles in southern sweden, 2020.

[11] NASA (National Aeronautics and Space Administration). Atmospheric aerosols: What are they, and why are they so important? `https://www.nasa.gov/centers/langley/news/factsheets/Aerosols.html`, 2017,[Online]. Visited 2022-10-08.

[12] S.C. Anenberg, J. Schwartz, D. Shindell, M. Amann, G. Faluvegi, Z. Klimont, G. Janssens-Maenhout, L. Pozzoli, R. Van Dingenen, E. Vignati, L. Emberson, N. Z. Muller, J.J. West, M. Williams, V. Demkine, W. K. Hicks, J. Kuylenstierna, F. Raes, and V. Ramanathan. Global air quality and health co-benefits of mitigating near-term climate change through methane and black carbon emission controls. *Environmental Health Perspectives*, 120(6):831–839, 2012.

[13] Z. Levin and W.R. Cotton (Eds.), editors. *Aerosol Pollution Impact on Precipitation: A Scientific Review*. Springer, 2009.

[14] IUPAC. Glossary of atmospheric chemistry terms (recommendations 1990). *Pure & Appl. Chem.*, 62(11):2167–2219, 1990.

[15] E. Bigg. Sources, nature and influence on climate of marine airborne particles. *Environmental Chemistry - ENVIRON CHEM*, 4, 01 2007.

[16] H. Zhuang, C.K. Chan, M. Fang, and A.S. Wexler. Size distributions of particulate sulfate, nitrate, and ammonium at a coastal site in hong kong. *Atmospheric Environment*, 33(6):843–853, 1999.

[17] J. Feichter and T. Leisner. Climate engineering: A critical review of approaches to modify the global energy balance. *The European Physical Journal Special Topics*, 176(1):81–92, 2009.

[18] Up in the aerosol. *Nature Geoscience*, 15(3), 2022.

[19] S. Szopa, V. Naik, B. Adhikary, P. Artaxo, T. Berntsen, W.D. Collins, S. Fuzzi, L. Gallardo, A. Kiendler-Scharr, Z. Klimont, H. Liao, N. Unger, and P. Zanis. Figure 6.13 in IPCC 2021:Short-Lived Climate Forcers. In Climate Change 2021: The Physical Science Basis. Contribution of Working Group I to the Sixth Assessment Report of the Intergovernmental Panel on Climate Change. In V. Masson-Delmotte, P. Zhai, A. Pirani, S.L. Connors, C. Péan, S. Berger, N. Caud, Y. Chen, L. Goldfarb, M.I. Gomis, M. Huang, K. Leitzell, E. Lonnoy, J.B.R. Matthews, T.K. Maycock, T. Waterfield, O. Yelekçi, R. Yu, and B. Zhou, editors, *IPCC 2021*, pages 817–922. Cambridge University Press, Cambridge, United Kingdom and New York, NY, USA, 2021.

[20] O. Boucher, D. Randall, P. Artaxo, C. Bretherton, G. Feingold, P. Forster, V.-M. Kerminen, Y. Kondo, H. Liao, U. Lohmann, P. Rasch, S.K. Satheesh, S. Sherwood, B. Stevens, and X.Y. Zhang. , 2013: Clouds and Aerosols. In: Climate Change 2013: The Physical Science Basis. Contribution of Working Group I to the Fifth Assessment Report of the Intergovernmental Panel on Climate Change . In T.F. Stocker, D. Qin, G.-K. Plattner, M. Tignor, S.K. Allen, J. Boschung, A. Nauels, Y. Xia, V. Bex, and P.M. Midgley, editors, *IPCC 2013*, pages 33–118. Cambridge University Press, Cambridge, United Kingdom and New York, NY, USA, 2013.

[21] B. J. Murray, D. O'Sullivan, J. D. Atkinson, and M. E. Webb. Ice nucleation by particles immersed in supercooled cloud droplets. *Chem. Soc. Rev.*, 41:6519–6554, 2012.

[22] A. Korolev, Greg Mcfarquhar, Paul Field, Charmaine Franklin, Paul Lawson, Z. Wang, E. Williams, S. Abel, Duncan Axisa, S. Borrmann, J. Crosier, Jacob Fugal, M. Krämer, Ulrike Lohmann, Oliver Schlenczek, and Manfred Wendisch. Mixed-phase clouds: Progress and challenges. *Meteorological Monographs*, 58:5.1–5.50, 06 2017.

[23] O. Boucher, D. Randall, P. Artaxo, C. Bretherton, G. Feingold, P. Foster, V.-M. Kerminen, Y. Kondo, H. Liao, U. Lohmann, P. Rasch, S. K. Satheesh, S. Sherwood, B. Stevens, and X. Y Zhang. 2013: Clouds and aerosols. in: Climate change 2013: The physical science basis. contribution of working group i to the fifth assessment report of the intergovernmental panel on climate change. Cambridge University Press, Cambridge, United Kingdom and New York, NY, USA., 2013.

[24] P. Forster, T. Storelvmo, K. Armour, W. Collins, J.-L. Dufresne, D. Frame, D.J. Lunt, T. Mauritsen, M.D. Palmer, M. Watanabe, M. Wild, and H. Zhang. Figure 7.7 in IPCC, 2021: Chapter 7. in: Climate change 2021: The Physical Science Basis. Contribution of Working Group I to the Sixth Assessment Report of the Intergovernmental Panel on Climate Change. In V. Masson-Delmotte, P. Zhai, A. Pirani, S.L. Connors, C. Péan, S. Berger, N. Caud, Y. Chen, L. Goldfarb, M.I. Gomis, M. Huang, K. Leitzell, E. Lonnoy, J.B.R. Matthews, T.K. Maycock, T. Waterfield, O. Yelekçi, R. Yu, and B. Zhou, editors, *IPCC 2021*, page 923–1054. Cambridge University Press, Cambridge, United Kingdom and New York, NY, USA, 2021.

[25] KIT (Karlsruhe Institute of Technology): Institute of Meteorology and Climate Research. Modes of ice nucleation. `https://www.imk-aaf.kit.edu/417.php`, [Online]. Visited 2023-03-14.

[26] G. Vali. Nucleation terminology. *Bull. Am. Meteorol. Soc.*, 66:1426–1427, 01 1985.

[27] C. Chou. *Investigation of ice nucleation properties onto soot, bioaerosol and mineral dust during different measurement campaigns*. PhD thesis, ETH Zürich, Zürich, Switzerland, 2011.

[28] ICOS (Integrated Carbon Observation System). Hyltemossa. `https://www.icos-sweden.se/hyltemossa`, [Online]. Visited 2023-01-10.

[29] Clouds ACTRIS (The Aerosol and Trace Gases Research Infrastructure). Hyltemossa. `https://www.actris.se/node/9`, [Online]. Visited 2023-01-10.

[30] Leckel (Sven Leckel Ingenieurbüro GmbH). Seq47/50-rv. `https://www.leckel.de/devices/seq4750-rv/`, 2014 [Online]. Visited 2023-01-10.

[31] Google. Location of hyltemossa research station situated in southern sweden. https://www.google.se/maps/place/Hyltemossa+Research+Station/@56.692346,12.7531276,7.75z/data=!4m6!3m5!1s0x4653e7339e32a287:0xefbbf5e3b81964eb!8m2!3d56.0978042!4d13.420146!16s%2Fg%2F11byyr92qs!5m1!1e4, [Online]. Visited 2023-01-18.

[32] M. Polen, T. Brubaker, J. Somers, and R. C. Sullivan. Cleaning up our water: reducing interferences from nonhomogeneous freezing of "pure" water in droplet freezing assays of ice-nucleating particles. *Atmospheric Measurement Techniques*, 11(9):5315–5334, 2018.

[33] J. K. F. Jakobsson, D. B. Waman, V. T. J. Phillips, and T. Bjerring Kristensen. Time dependence of heterogeneous ice nucleation by ambient aerosols: laboratory observations and a formulation for models. *Atmospheric Chemistry and Physics*, 22(10):6717–6748, 2022.

[34] A. F. Stein, R. R. Draxler, G. D. Rolph, B. J. B. Stunder, M. D. Cohen, and F. Ngan. Noaa's hysplit atmospheric transport and dispersion modeling system. *Bulletin of the American Meteorological Society*, 96(12):2059–2077, 2015.

[35] T. Kabir. *Seasonal Variability of Ice Nucleating Particles (INP) in Southern Sweden*. PhD thesis, University of Gothenburg, Sweden, 2022.

[36] Naturhistoriska riksmuseet. Pollengrafer hässleholm 2021. https://pollenrapporten.se/prognoser/hassleholm/pollengrafer2021.4.315eb1f6175f62b587e8682.html, 2021 [Online]. Visited 2023-04-30.

[37] W.R. Ott. A physical explanation of the lognormality of pollutant concentrations. *Journal of the Air & Waste Management Association*, 40(10):1378–1383, 1990.

[38] P. J. DeMott, A. J. Prenni, X. Liu, S. M. Kreidenweis, M. D. Petters, C. H. Twohy, M. S. Richardson, T. Eidhammer, and D. C. Rogers. Predicting global atmospheric ice nuclei distributions and their impacts on climate. *Proceedings of the National Academy of Sciences*, 107(25):11217–11222, 2010.

[39] J. Schneider, K. Höhler, P. Heikkilä, J. Keskinen, B. Bertozzi, P. Bogert, T. Schorr, N. S. Umo, F. Vogel, Z. Brasseur, Y. Wu, S. Hakala, J. Duplissy, D. Moisseev, M. Kulmala, M. P. Adams, B. J. Murray, K. Korhonen, L. Hao, E. S. Thomson, D. Castarède, T. Leisner, T. Petäjä, and O. Möhler. The seasonal cycle of ice-nucleating particles linked to the abundance of biogenic aerosol in boreal forests. *Atmospheric Chemistry and Physics*, 21(5):3899–3918, 2021.

A

Meteorological parameters and Aerosol properties

The meteorological and aerosol data used in Figure 5.4 has been individually plotted against the month to show the variability during the time period used.

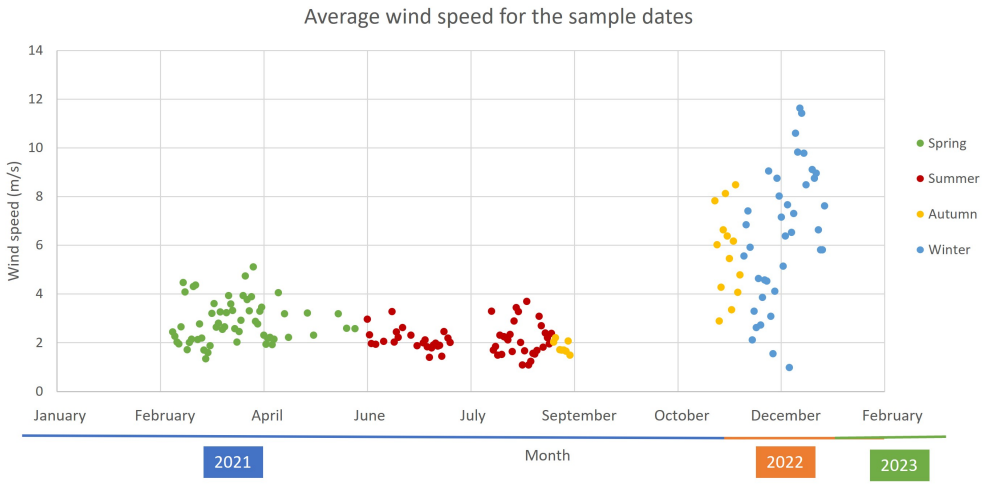

Figure A.1: A time series of the average wind speed at Hyltemossa research station for the filter sample dates analysed. Where the year for each month is shown in the x-axis as a coloured line.

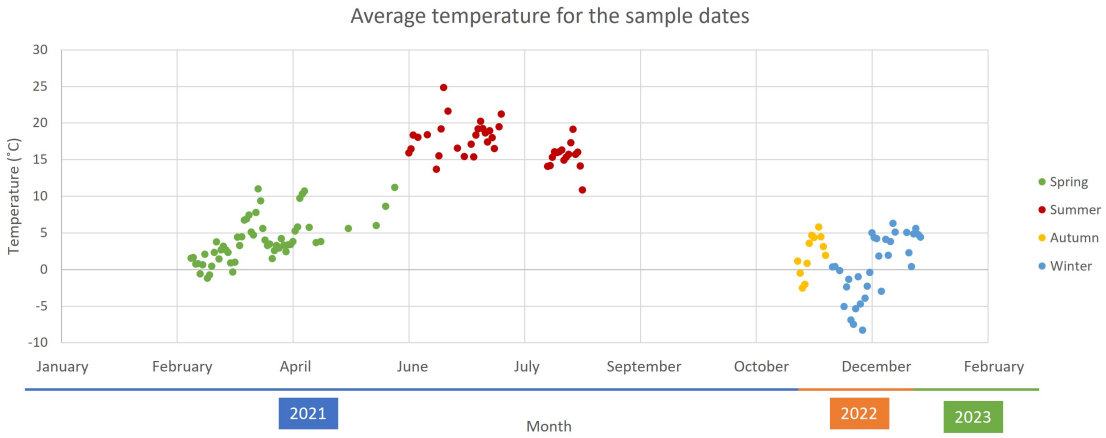

Figure A.2: A time series of the average temperature at Hyltemossa research station for the filter sample dates analysed. Where the year for each month is shown in the x-axis as a coloured line.

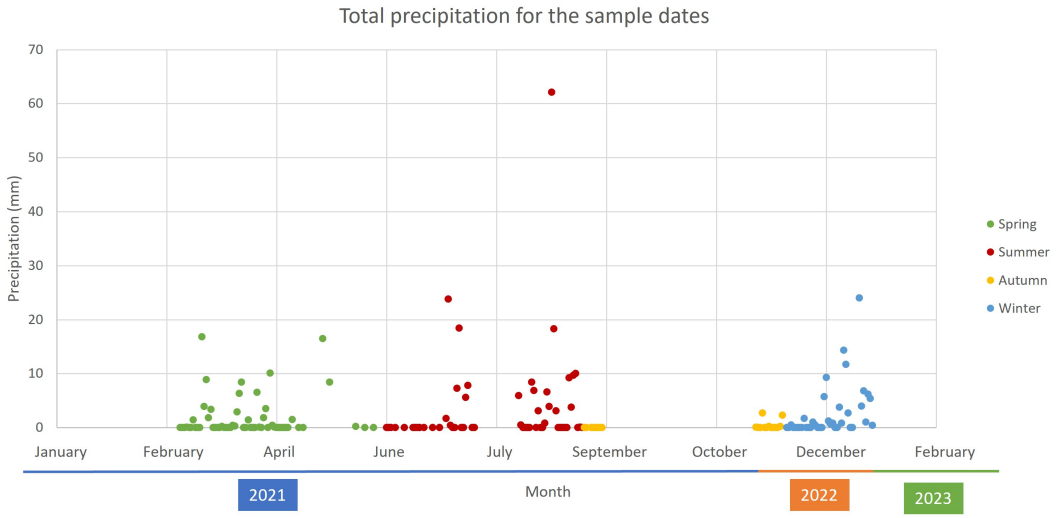

Figure A.3: A time series of the total amount of precipitation at Hyltemossa research station for the filter sample dates analysed. Where the year for each month is shown in the x-axis as a coloured line.

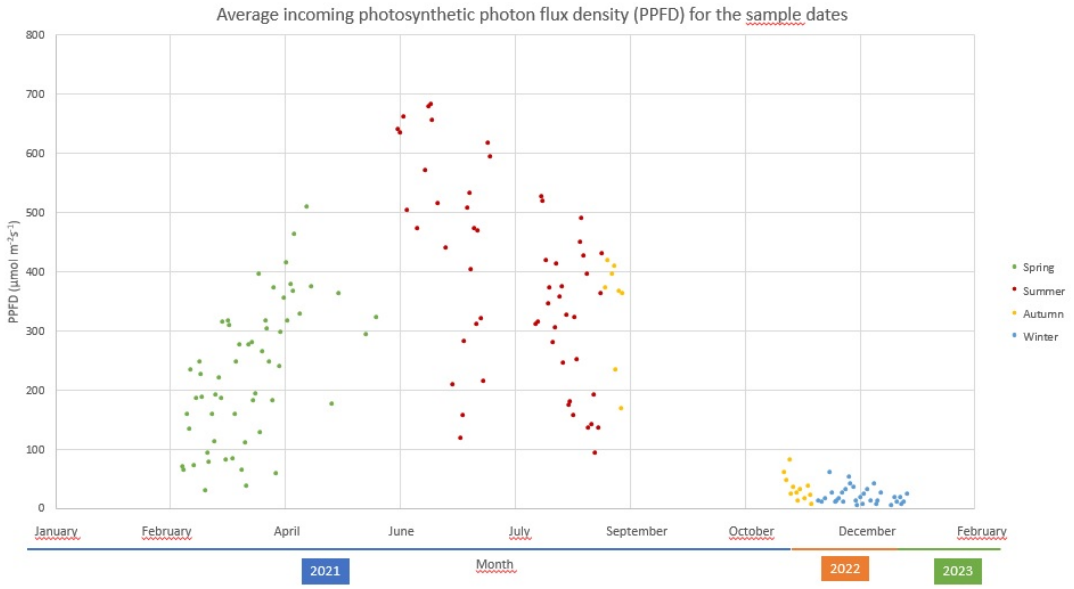

Figure A.4: A time series of the photosynthetic photon flux density at Hyltemossa research station for the filter sample dates analysed. Where the year for each month is shown in the x-axis as a coloured line.

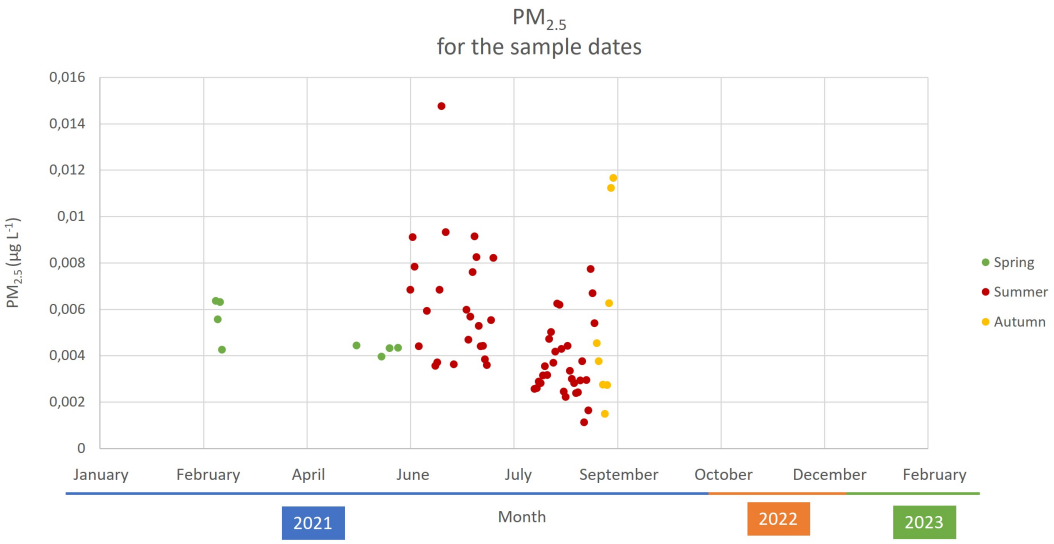

Figure A.5: A time series of the $PM_{2.5}$ at Hallahus for the filter sample dates analysed. Where the year for each month is shown in the x-axis as a coloured line.

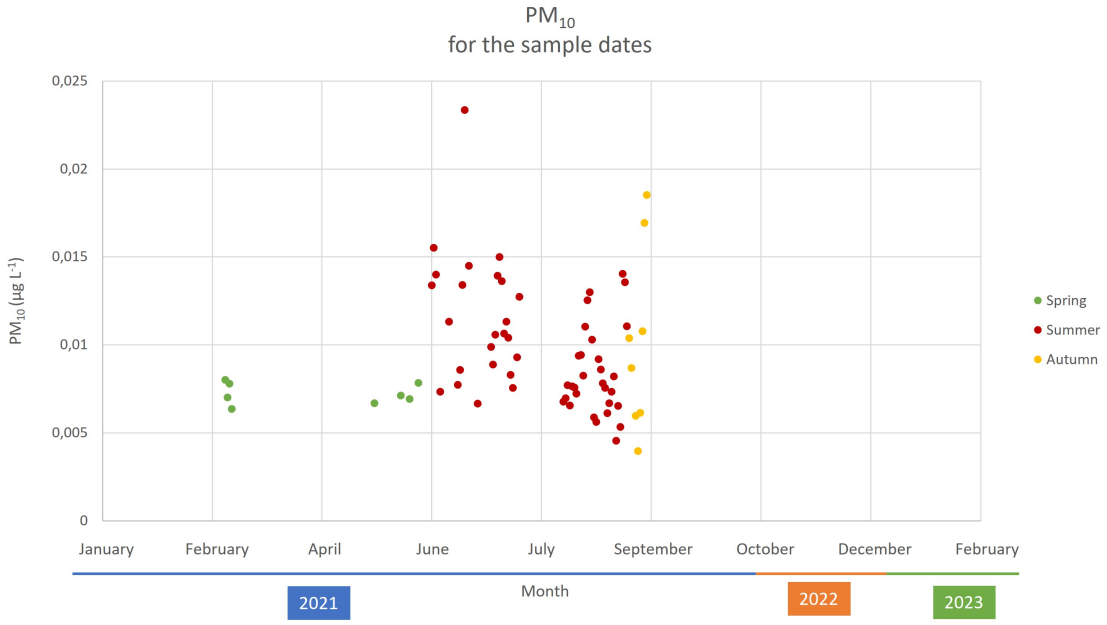

Figure A.6: A time series of the PM_{10} at Hallahus for the filter sample dates analysed. Where the year for each month is shown in the x-axis as a coloured line.

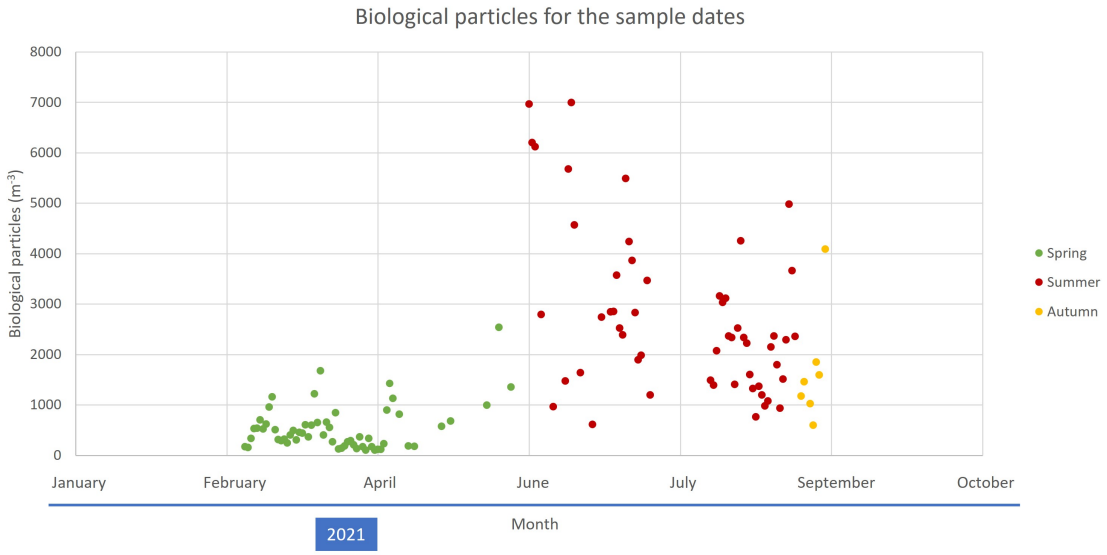

Figure A.7: A time series of the biological particles at Hyltemossa research station for the filter sample dates analysed. Where the year for each month is shown in the x-axis as a coloured line.

B

Freezing spectras

Figure B.1 to Figure B.5 shows the freezing spectras for each of the sampled months. Each line is a sample filter date and from these the highest respective lowest freezing temperature for each month can be determined. These high and low days of each months are the ones that are used in the back trajectories of Figure 5.9 and Figure 5.10.

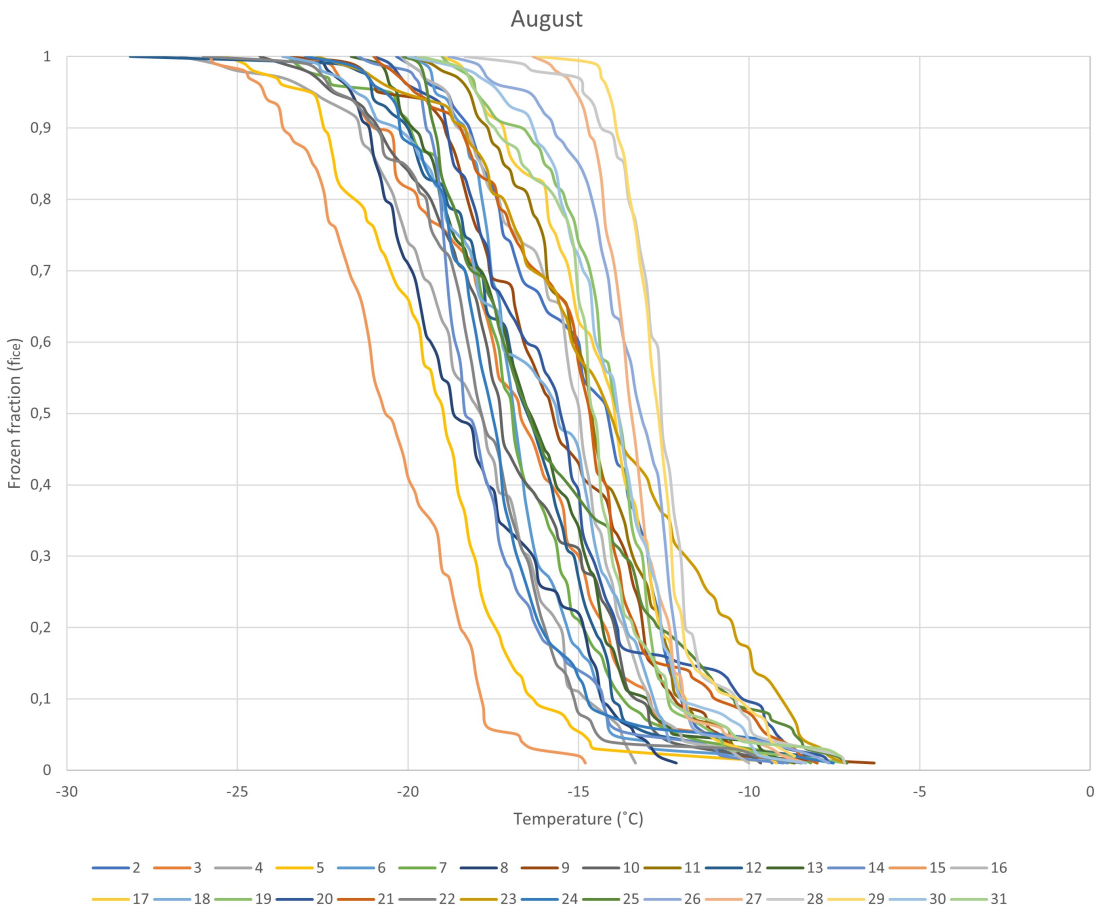

Figure B.1: Shows the freezing spectra of the month of August 2021 where all the filter sample dates are plotted. From this the highest and lowest freezing temperature can be determined.

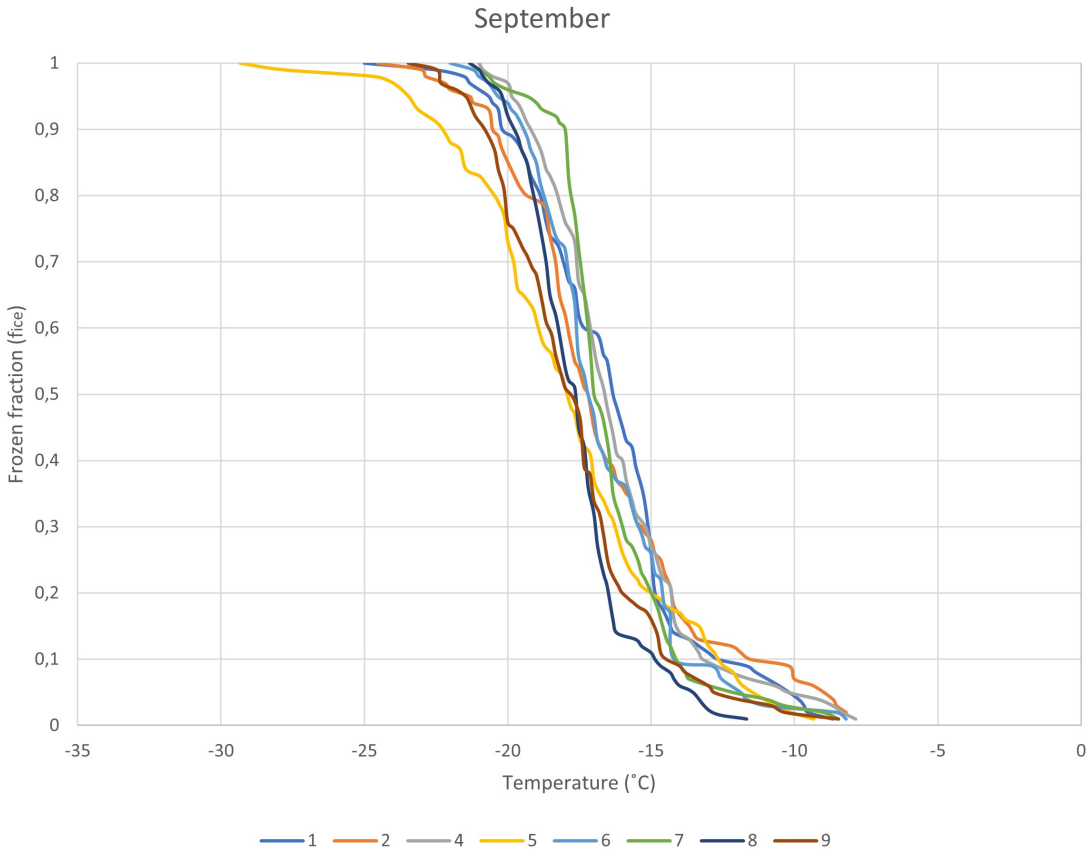

Figure B.2: Shows the freezing spectra of the month of September 2021 where all the filter sample dates are plotted. From this the highest and lowest freezing temperature can be determined.

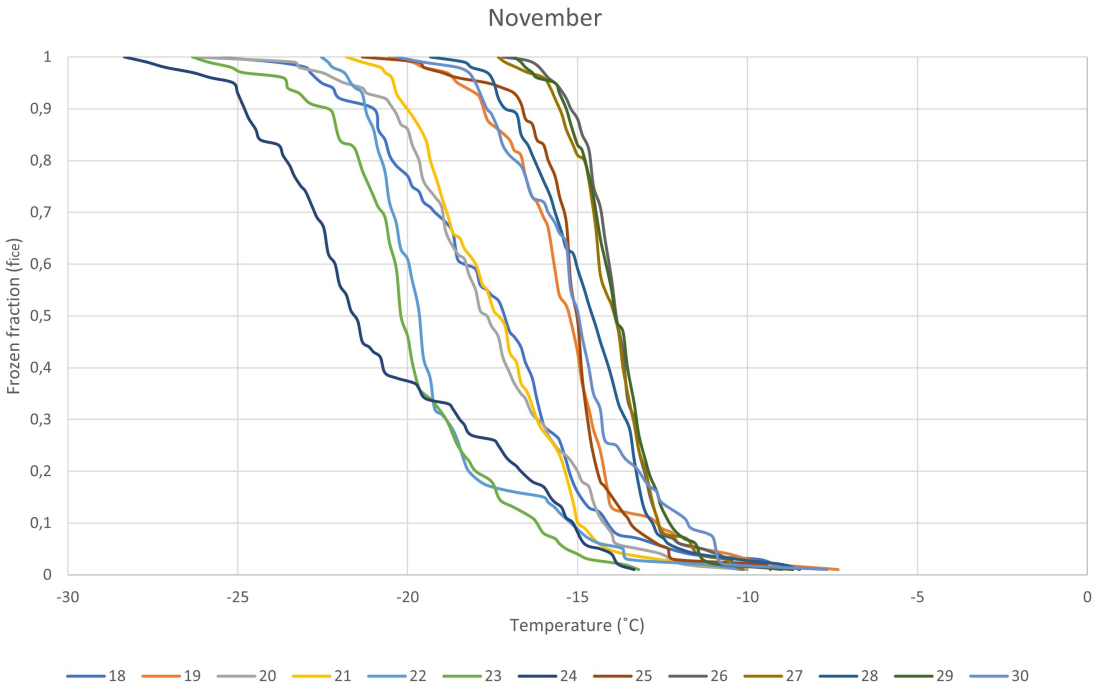

Figure B.3: Shows the freezing spectra of the month of November 2022 where all the filter sample dates are plotted. From this the highest and lowest freezing temperature can be determined.

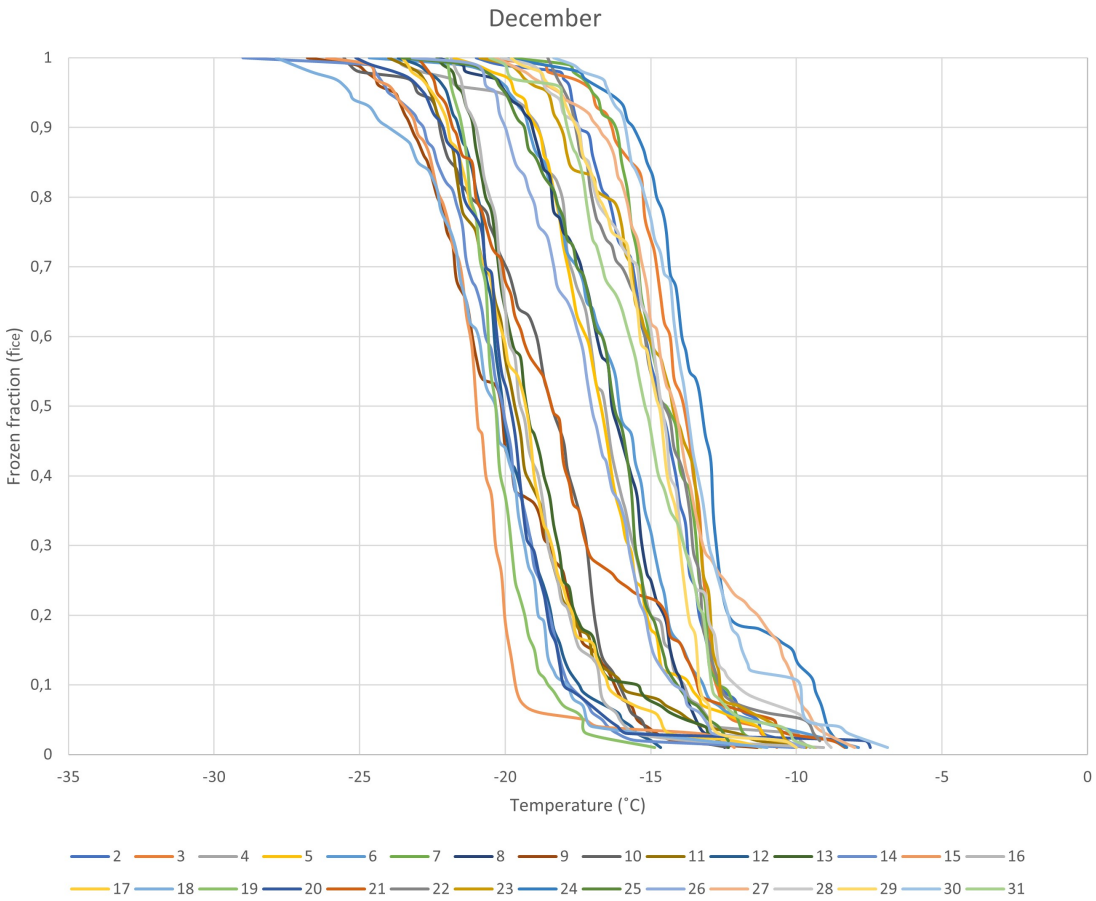

Figure B.4: Shows the freezing spectra of the month of December 2022 where all the filter sample dates are plotted. From this the highest and lowest freezing temperature can be determined.

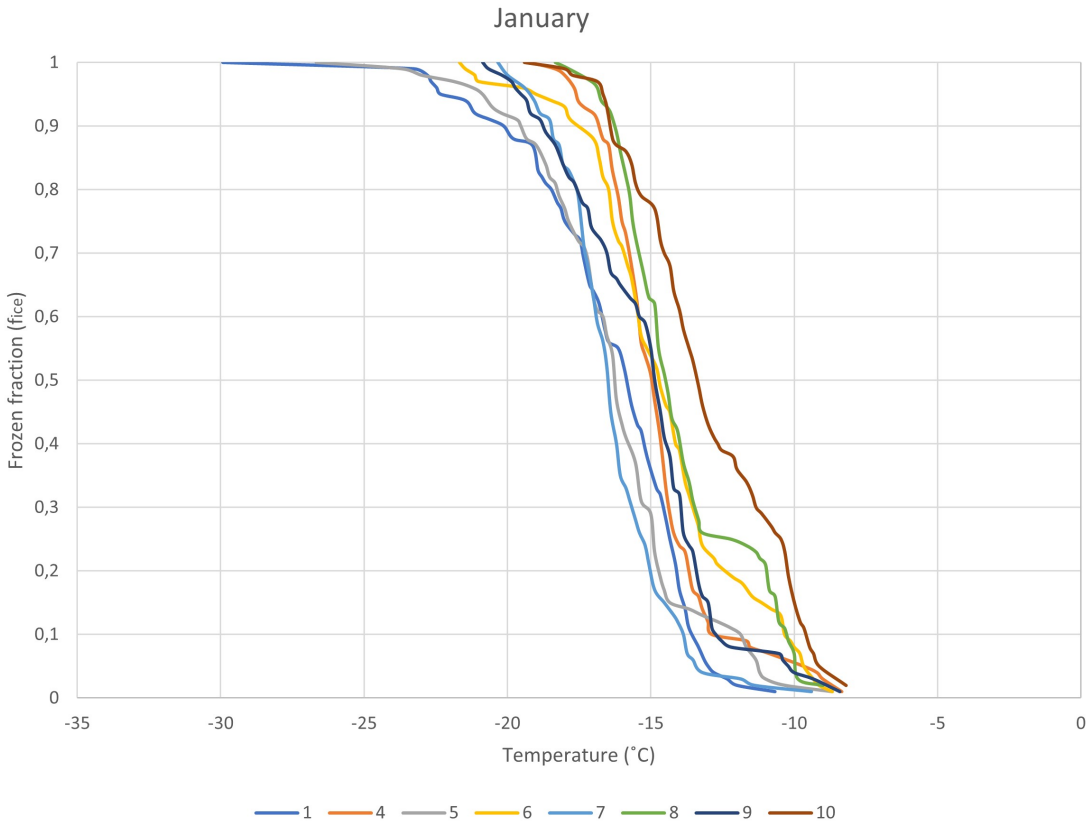

Figure B.5: Shows the freezing spectra of the month of January 2023 where all the filter sample dates are plotted. From this the highest and lowest freezing temperature can be determined.

Investigation of Ice Nucleating Particles (INPs) in southern Sweden

With a special focus on their origin, possible connection to meteorological parameters and aerosol properties

Malin Forsmalm
Department of Biological and Environmental Sciences